ISSN 1590-2595
Anno 2015_Numero 129

Use of Multiple in situ and remote sensing instruments and techniques at Solfatara field campaign for measurements of CO_2, H_2S and SO_2 emissions: special demonstration on unmanned aerial systems

Quaderni di Geofisica

129

Istituto Nazionale di Geofisica e Vulcanologia

Quaderni di Geofisica

Segreteria di Redazione
Francesca Di Stefano - Referente
Rossella Celi
Tel. +39 06 51860068
redazionecen@ingv.it

in collaborazione con:
Barbara Angioni (RM1)

REGISTRAZIONE AL TRIBUNALE DI ROMA N.174|2014, 23 LUGLIO

Sede legale: Via di Vigna Murata, 605 | Roma

ISSN 1590-2595
Anno 2015_Numero 129

Use of Multiple in situ and remote sensing instruments and techniques at Solfatara field campaign for measurements of CO_2, H_2S and SO_2 emissions: special demonstration on unmanned aerial systems

Utilizzo di strumentazione ed applicazioni in situ e prossimali durante la campagna di misure di CO_2, H_2S e SO_2 presso la Solfatara: applicazione ad un drone

Malvina Silvestri[1], Jorge Andres Diaz[2], Enrica Marotta[3], Massimo Musacchio[1], Maria Fabrizia Buongiorno[1], Fabio Sansivero[3], Carlo Cardellini[4], David Pieri[5], Stefania Amici[1], Emanuela Bagnato[4], Giulio Beddini[4], Pasquale Belviso[3], Antonio Carandente[3], Laura Colini[1], Fawzi Doumaz[1], Rosario Peluso[3], Claudia Spinetti[1]

[1]**INGV** (Istituto Nazionale di Geofisica e Vulcanologia, Centro Nazionale Terremoti)

[2]**GASLAB, CICANUM** (Università del Costa Rica, San Josè, Costa Rica)

[3]**INGV** (Istituto Nazionale di Geofisica e Vulcanologia, Sezione di Napoli - Osservatorio Vesuviano)

[4]**Università degli Studi di Perugia** (Dipartimento di Fisica e Geologia)

[5]**JPL** (Jet Propulsion Laboratory of the California Institute of Technology, Pasadena, CA, USA)

in copertina Bocca Nuova: la fumarola. Foto di Francesco "Ciskie" Malafarina (particolare)

Use of Multiple in situ and remote sensing instruments and techniques at Solfatara field campaign for measurements of CO_2, H_2S and SO_2 emissions: special demonstration on unmanned aerial systems

In this paper we present the field campaign held in October at the Solfatara of Pozzuoli, near Naples, concerning measurements of CO_2, H_2S and SO_2. The campaign was carried out in collaboration with the University of Costa Rica and Jet Propulsion Laboratory of the California Institute of Technology (Pasadena, California) and has allowed the acquisition of a number of measures through scientific instrumentation as miniaturized multi-gas, thermal cameras and spectro-radiometer. First analysis in terms of brightness temperature was carried out through Landsat and ASTER satellite data. In addition to the instrumental test, one of the objectives has been to verify the possibility of mounting a light payload on a quadcopter and fly it on areas of high gas flow to allow the acquisition of data security. First results are reported in this work while it is foreseen a more accurate analysis of the data obtained.

In questo lavoro viene presentata la campagna di misure di CO_2, H_2S e SO_2 svoltasi nel mese di ottobre presso la Solfatara di Pozzuoli, vicino Napoli. La campagna è stata svolta in collaborazione con l'Università di Costa Rica e il Jet Propulsion Laboratory del California Institute of Technology (Pasadena, California) ed ha permesso l'acquisizione di diverse misure attraverso strumentazione scientifica come multigas miniaturizzati, camere termiche, spettroradiometri. Una prima analisi in termini di temperatura di brillanza è stata effettuata attraverso i dati satellitari come Landsat e ASTER. Tra gli obiettivi, oltre il test strumentale, è stata verificata la possibilità di montare un payload leggero su un quadcopter e farlo volare su aree ad elevato flusso di gas per permettere l'acquisizione di dati in sicurezza. I primi risultati sono esposti in questo lavoro mentre è in corso un'analisi più accurata dei dati ottenuti.

Introduction

Aim of this work is the description of field campaign at the Solfatara of Pozzuoli near Naples, in late October 2014. The campaign, anticipated by a seminar held at the INGV in Naples on October 29, was conducted in collaboration with INGV staff (Rome and Naples), Dr. Jorge Andres Diaz of the University of Costa Rica and Dr. David Pieri of the Jet Propulsion Laboratory of the California Institute of Technology (Pasadena, California).

Part of the results were obtained using a miniature multigas payload and a small mass spectrometer based unmanned aerial system (UAS) instrument, both developed for in situ volcanic emissions measurements, providing volcanic CO_2, H_2S and SO_2 measurement. Surface temperature measurements through thermal camera and thermocouples are also reported. To complete the analysis conducted during the campaign, some results using the spectro-radiometer ASD FieldSpec of optical laboratory of "Unità Funzionale Dati satellitari per l'osservazione della Terra" (UF8) are also reported. A comparison with remote sensor data acquired by Landsat 8 and ASTER will be done in the next months, while in this paper a brief description on the Landsat 8 data acquired on 27 October and ASTER data acquired 26 September are reported.

1. Objective of field campaign

The Solfatara of Pozzuoli, near Naples, is part of the Campi Flegrei volcanic complex that contains a fumarolic field more or less extended, whose activity is mainly from the release of steam and gases with high sulphur component.

The Solfatara of Pozzuoli is located within an area densely

populated and historically had different periods of activity; the latest explosive activity dates back to 1538 (built of Monte Nuovo) [Rosi and Santacroce, 1984; Vito et al., 1987; Rosi and Sbrana, 1987].

The Campi Flegrei is also characterized by periodically bradyseism whose most recent crisis are those of 1969-1972 and 1982-1984. During the latter period a maximum lift height of about 1.8 m and several thousands of shallow earthquakes (<4 km) were recorded and caused the evacuation of about 40,000 people. [Barberi et al., 1984]. Coinciding with this period of uplift the opening of a fracture has also recorded, oriented towards approximately NE-SW, about 0.7 m wide within the Solfatara itself [Rosi and Sbrana, 1987].

The campaign was held on the 30th and 31th October 2014 and had the main objective to test the miniaturized instruments developed for NASA under ROSES project*: "ASTER remote sensing calibration and validation using In situ UAS based measurements of volcanic plume emissions"* directed by Dr. Pieri from JPL as PI and Dr. Diaz from University of Costa Rica as Co-I. Dr. Buongiorno from INGV has also serve as a collaborator to this project and provided the logistics to conduct the testing in Naples, Italy. These instruments were ground tested in Costa Rica by the Universidad de Costa Rica sensor characterization lab (GasLab) using different platforms aiming to measure in situ gaseous emissions with a multi scale approach from airborne drones, tethered balloons and ground measurements to calibrate space borne remote sensing measurements. To complete the instrument tests, the multigas payload was attached to an small *quadcopter* and flown into the Solfatara Volcano fumarolic areas, demonstrating the possibility to attach a light payload on small *quadcopter* and fly on areas with high gas flow to allow the safe acquisition of volcanic emissions data.

The primary goal has been the testing of these instruments at the Solfatara Volcano in order to improve the understanding of the chemical and physical properties of emissions for mitigation of local volcanic hazards, for the validation of species detection and abundance of retrievals based on remote sensing, and to validate transport models.

1.1 CO_2, H_2S and SO_2 measurements

Technological growth in the field of small unmanned aircraft systems and their integration with a variety of multigas sensors instruments (such as miniature mass spectrometer) or single specie sensors (such as electrochemical and IR sensors), have enhanced the possibilities and applications of what are now called unmanned aircraft systems. With this technology, it is possible to perform monitoring measurements of volcanic activity without risking the lives of scientists and personnel performing analysis during the field campaigns in areas of high volcanic activity and can be considered to support to the calibration and validation of satellite

Figure 1 MiniGas D_α Field Test Unit for CO_2, SO_2 e H_2S, T, P, RH and GPS telemetered in situ measurements.
Figura 1 MiniGas D_α Field Test Unit per misure in situ di CO_2, SO_2 e H_2S, T, P, RH e GPS.

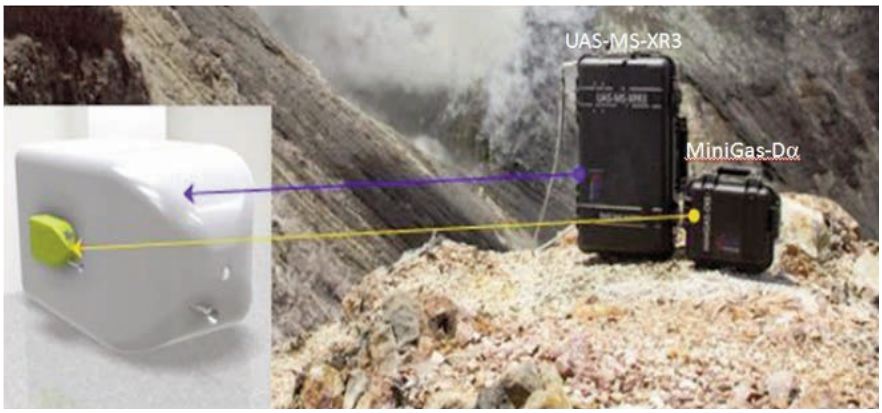

Figure 2 UAV-MS-XPR3 Mass Spectrometer for multiple gas analysis and MiniGas payload (UAS airborne configuration in left, ground test units on right).
Figura 2 Spettrometro di massa per analisi di specie gassose e MiniGas payload (configurazione UAS a sinistra, unità di test a terra a destra).

data measurements. These systems allowed the acquisition of real-time information such as temperature, pressure, relative humidity, SO_2, H_2S, CO_2, and GPS geolocation. The acquired data are both stored in the sensor and transmitted to a computer for real time viewing information. Information can be returned in the form of 3D concentration maps.

The equipment used during the campaign at Solfatara Volcano were the MiniGas D_α payload (Figure 1) and the UAV-MS-XPR3 Mass Spectometer ground test instrument (Figure 2). The MiniGas is a low cost 500 gr experimental payload and allowed the acquisition of both 2D ground fumarolic emissions using a hand portable case and 3D airborne CO_2 and H_2S concentration maps using a DJI Phantom Vision 2 *quadcopter* from which the sensor package was tethered (Figure 3).

The MiniGas is a multisensor instrument based on an Arduino platform developed by Dr Diaz and includes temperature, pressure, relative humidity, SO_2 and H_2S electrochemical sensors, an non-dispersing near infrared CO_2 sensor, GPS sensor, onboard data storage and telemetry via Xbee Pro antennas. It has been flight tested within the Turrialba volcanic plume onboard the VECTOR WING 100 UAV [Diaz et al., 2013] and tethered balloon airborne platforms, generating real time 3D gas concentration plots of the active volcanic plumes. In situ sampling with the MiniGas is achieved by injecting an airstream into the multi sensor platform with a very small displacement pump (1.2 lpm) to generate a concentration profile.

Figure 3 MiniGas Dragon - UAV Test Unit mounted on DJI Phatom Vision 2 *Quadcopter*.
Figura 3 MiniGas Dragon - UAV Test Unit istallato sul DJI Phatom Vision 2 *Quadcopter*.

Figure 4 Image acquired by *Quadcopter* during the field campaign; in the two boxes the Bocca Grande and Bocca Nuova sites.
Figura 4 Immagine acquisita dal *Quadcopter* durante la campagna di misura; nei due riquadri i siti Bocca Grande e Bocca Nuova.

The UAV-MS-XPR3 tested at Solfatara is based on the Transpector XPR3 mass spectrometer, which is the latest generation of high-pressure, quadrupole-based process gas analysis mass spectrometer capable of operation in the mTorr (10-3 Torr) vacuum range and is the smallest miniature commercial MS suited to volcanic gas analysis. The miniature ion source and quadrupole can operate from UHV to 20 mTorr and a specially designed electron multiplier (EM) will operate up to 10 mTorr. The XPR3 is well suited for portable MS when paired with a small turbo pump (e.g. Pfeiffer Vacuum's TPD 11 or Creare LLC MDP). It is 14.3 x 12.4 x 17.5 cm in dimensions and just over 1 kg. The Transpector XPR3 is controlled using INFICON's FabGuard Suite of software loaded into a single board computer (Fit PC3) to acquire the MS and MiniGas, data, store, and transmit the data.

The DJI Phantom Vision 2 *quadcopter* is a complete aerial camera system that is ready to fly within minutes. It carries an extremely high quality stills camera and a 4GB micro SD card, shoots full HD video at 1080p 30/60i and takes 14 megapixel still photos. The integrated GPS auto-pilot system offers position holding and provides altitude lock along with stable hovering giving constant stable flights so it can focus on getting the shots. In the http://www.dji.com/product/phantom-2-vision/spec website the *quadcopter* technical features are reported. This radio-controlled *quadcopter* has features like a battery powered (compared to competing models) that lasts 25 minutes and has a range acceptable given the 10/15 minutes of competitors. In Figure 4 the image acquired by DJI Phantom Vision 2 *quadcopter* during the field campaign is showed.

Examples of 3D H_2S and CO_2 measurements acquired on the Solfatara are reported in Figure 5 and Figure 6. The Dragon MiniGas was led by land through the *quadcopter* close the most active fumaroles.

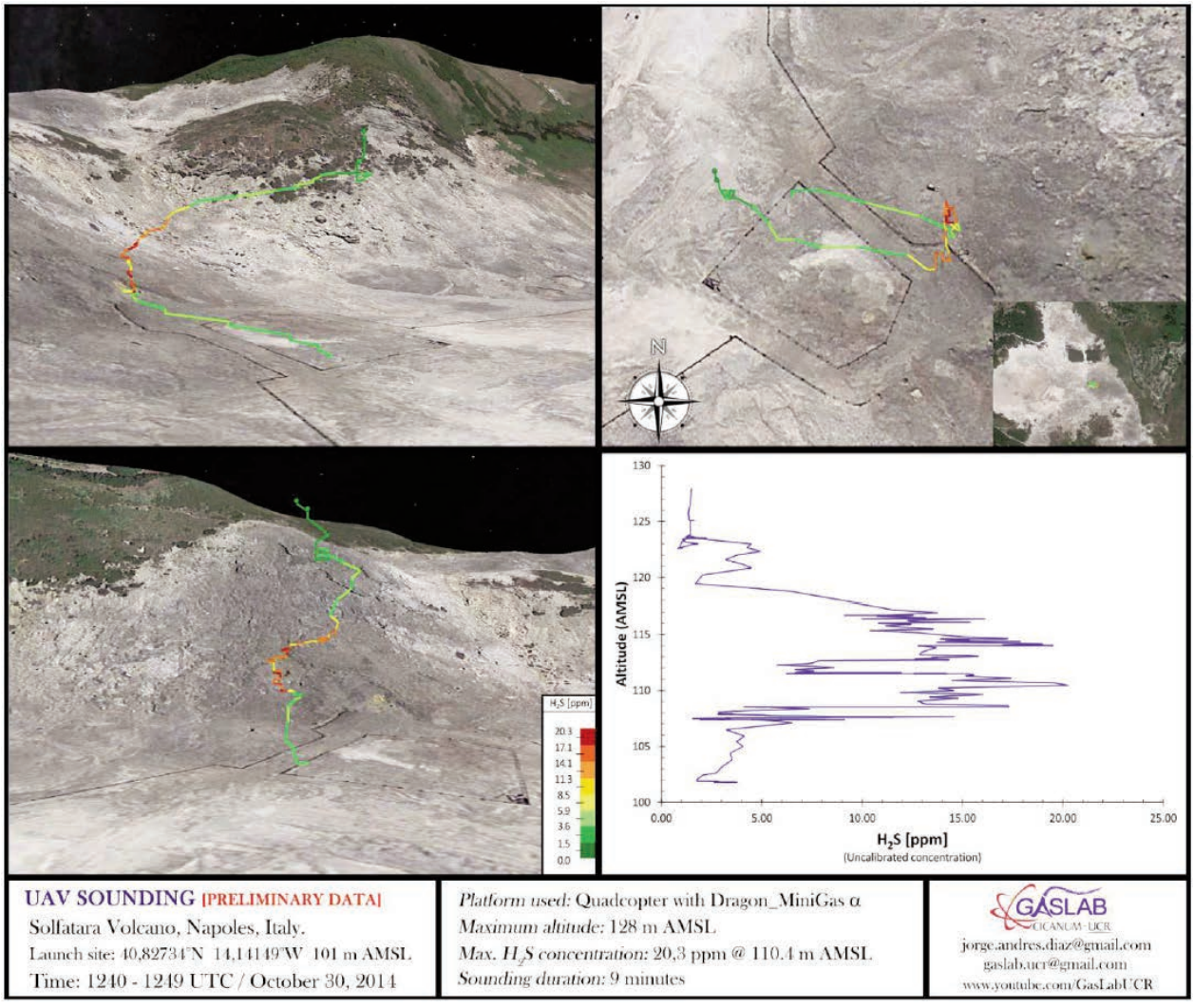

Figure 5 3D view of H_2S concentration. The graph in the lower right shows the trend of the concentration of H_2S as a function of the height. Trajectories in Google Earth™ images are colour-coded according to the legend on the left.
Figura 5 Mappa 3D della concentrazione di H_2S. Il grafico in basso a destra riporta l'andamento della concentrazione di H_2S in funzione dell'altezza. Il profilo verticale della concentrazione di H_2S è riportato su Google Earth™ e la scala di colori riporta il valore della concentrazione di H_2S.

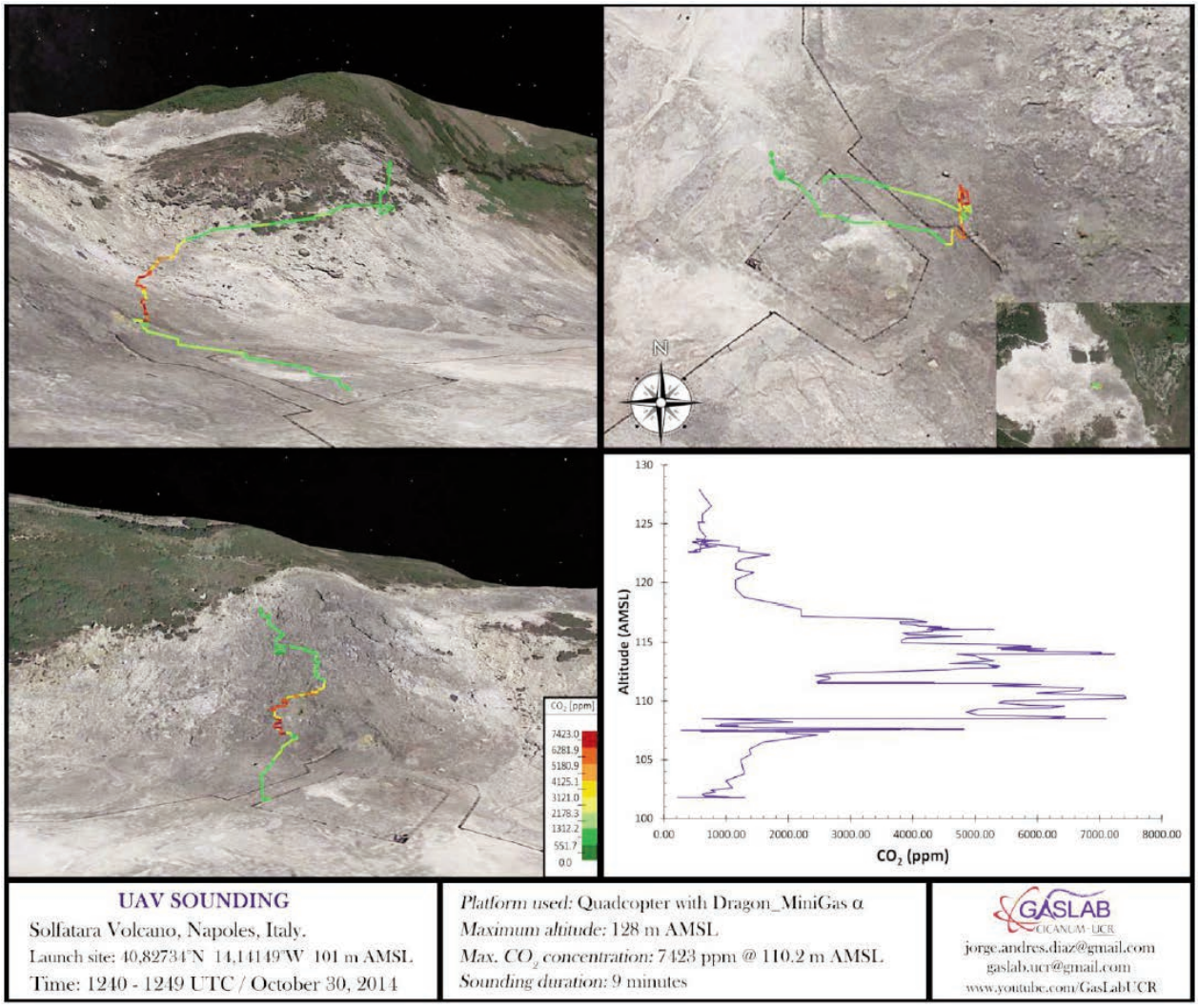

Figure 6 3D view of CO_2 concentration. The graph in the lower right shows the trend of the concentration of CO_2 as a function of the height. Trajectories in Google Earth™ images are colour-coded according to the legend on the left.
Figura 6 Mappa 3D della concentrazione di CO_2. Il grafico in basso a destra riporta l'andamento della concentrazione di CO_2 in funzione dell'altezza. Il profilo verticale della concentrazione di CO_2 è riportato su Google Earth™ e la scala di colori riporta il valore della concentrazione di H_2S.

Figure 7 to Figure 9 show more results of measurements collected with the MiniGas payload attached to *quadcopter* obtaining CO_2 and H_2S concentration as a function of time, altitude. Temperature, humidity and pressure were also collected and plotted.

In Figure 7 all parameters (H_2S concentration, CO_2 concentration, RH% and Temperature) increase when the Quadcopter flies below, inside and above the fumarolic plume and intersecting the plume. In Figure 8 high water vapor concentration is indicative when instrument penetrates the fumarolic plume. Data show very good correlation between water vapor and H_2S and CO_2 gas concentration (increasing water vapor we have increasing volcanic gas concentration). In Figure 9 data show very good correlation between the H_2S and CO_2 gas concentration signal which demonstrates the drone penetrates the plume and is able to do a quick characterization of the volcanic plume.

Finally, in situ measurements of CO_2, SO_2 and H_2S using the MS mass spectrometer system (Figure 10) were collected at the Bocca Nuova Fumarole. The measurement of gas sample is pulled in by a small 4 lpm diaphragm pump and sample is introduced to MS vacuum chamber via 2 critical orifices. For fumarole sampling a water vapor bypass is set before the inlet is remove the high water vapor content. A new experiment will set for September next year to test for gases with and without the bypass.

Figure 11 shows the in situ mass spectra of gases emitted at Solfatara Bocca Nuova fumarole during the deployment. The MS analysis shows the presence of H_2O and CO_2 as main gases emitted and reveals the presence of H_2S as trace gas and SO_2 in low ppm concentration (besides air contamination for N_2, O_2, Ar peaks). SO_2 was detected by mass spec-

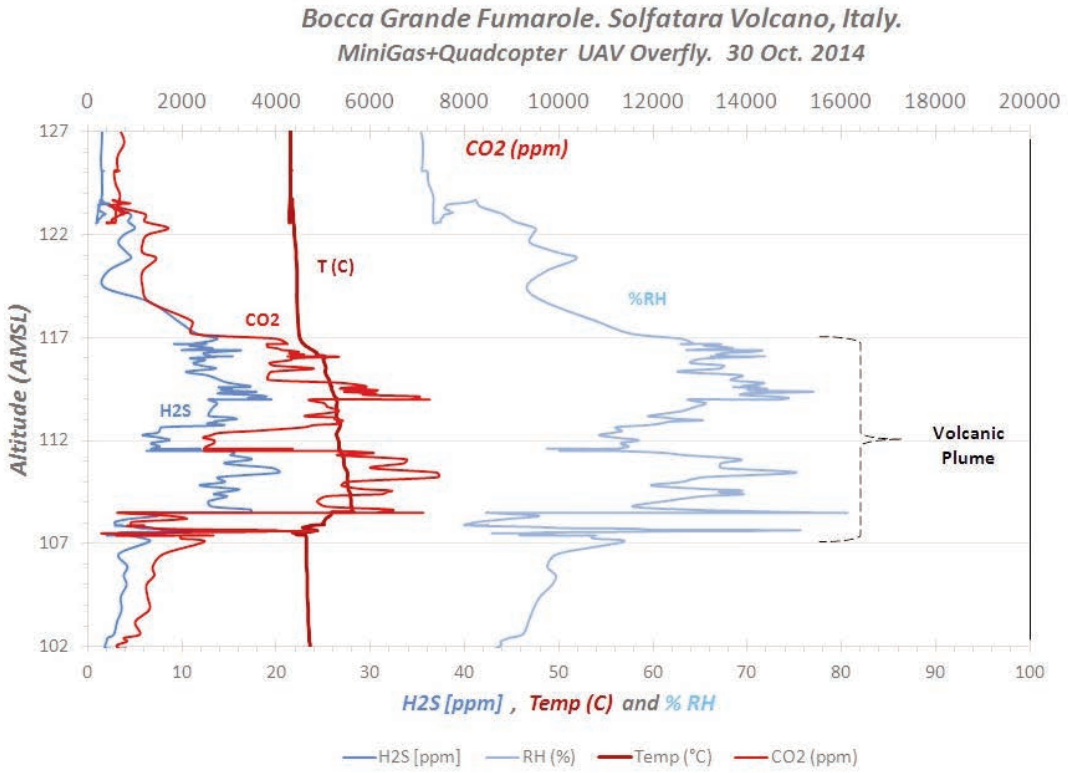

Figure 7 Solfatara plume characterization using MiniGas instrument attached to DJI Quadcopter Drone.
Figura 7 Caratterizzazione del plume di Bocca Grande attraverso MiniGas istallato sul DJI Quadcopter Drone.

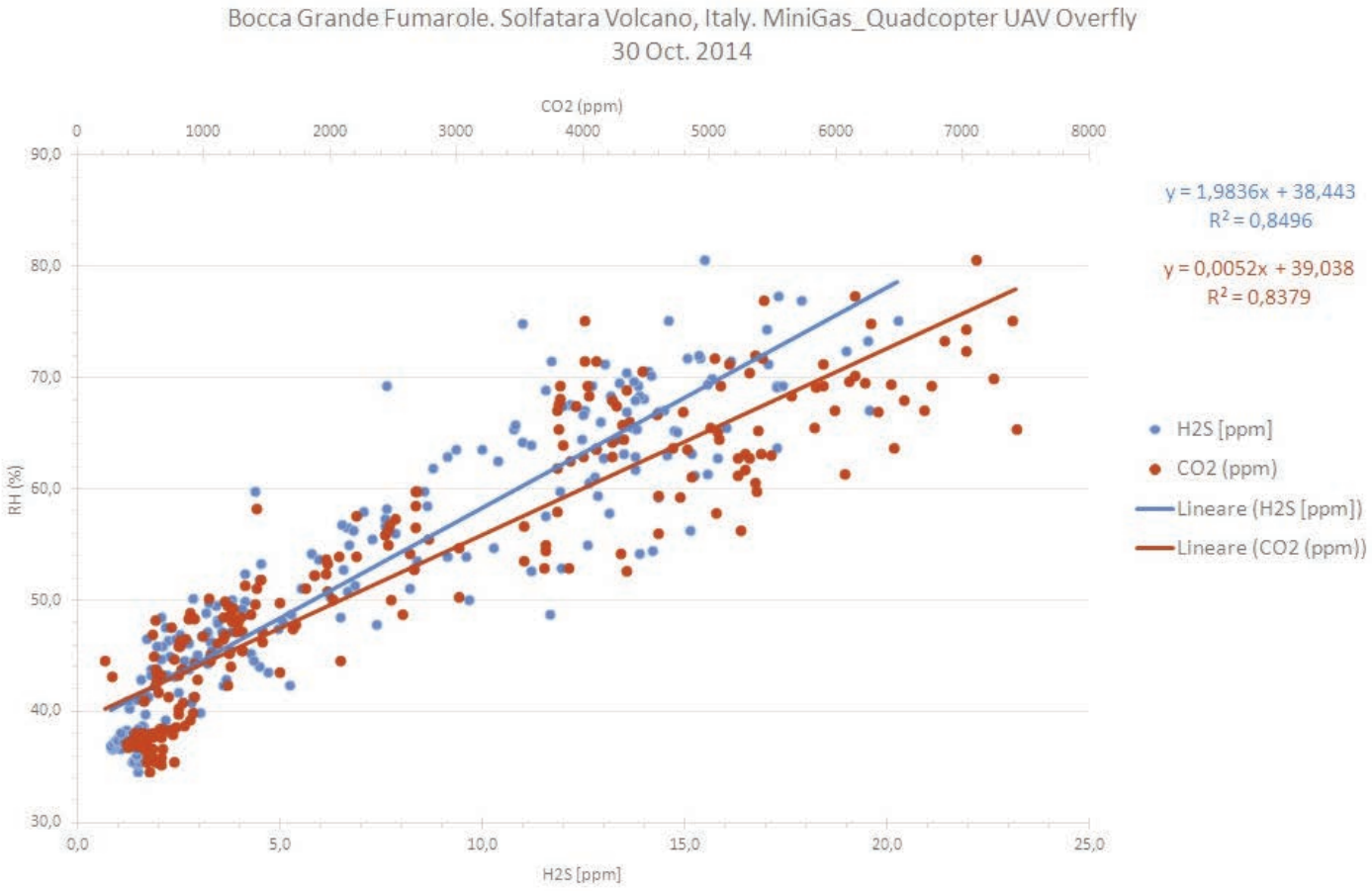

Figure 8 Solfatara plume characterization correlating gas concentrations to relative humidity.
Figura 8 Correlazione tra la concentrazione di CO_2 e H_2S vs umidità relativa.

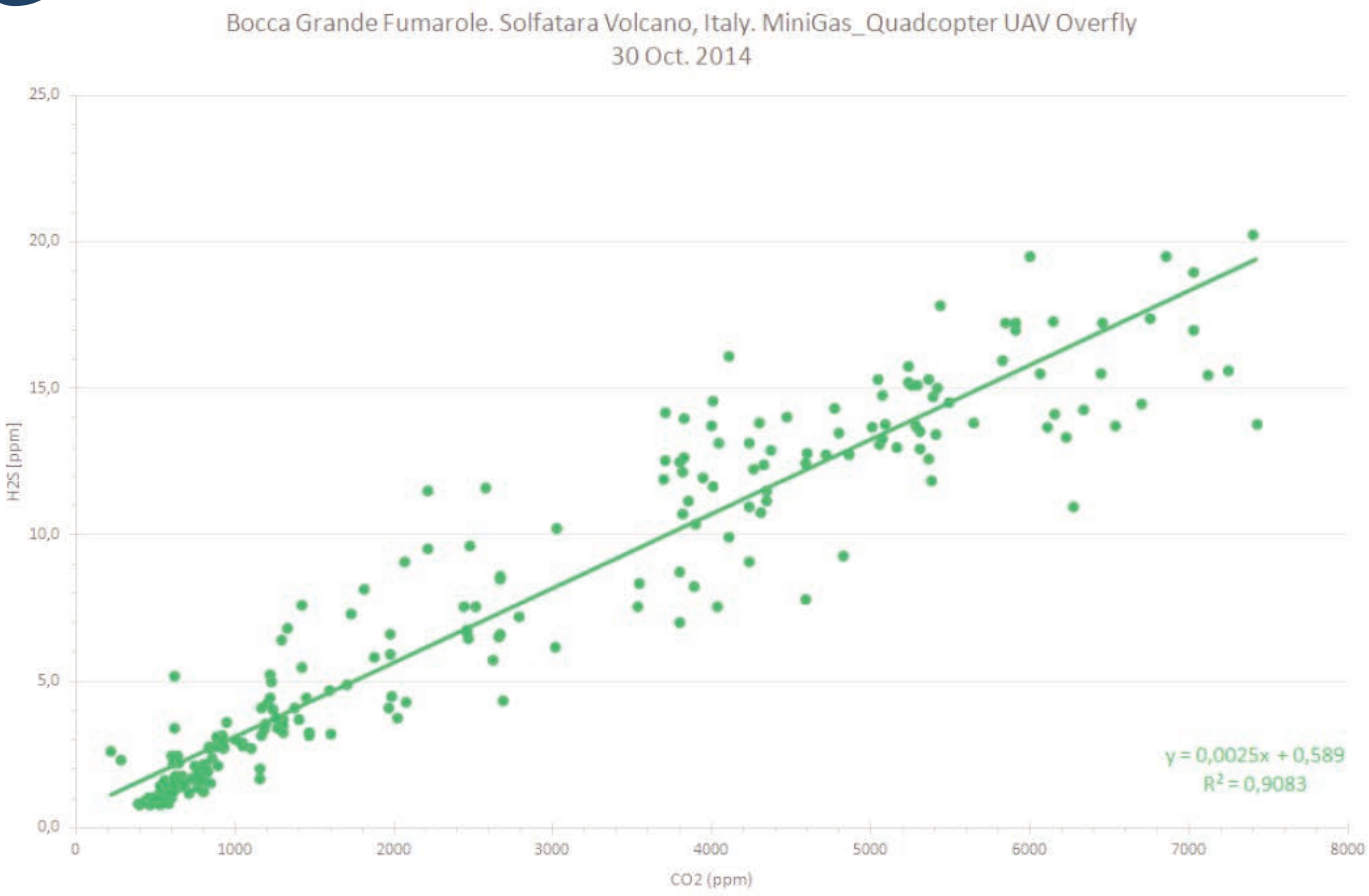

Figure 9 Solfatara plume characterization correlating volcanic gas concentrations of H_2S vs CO_2.
Figura 9 Correlazione tra la concentrazione di H_2S vs CO_2.

Figure 10 In situ Mass Spectometer gas analysis at Bocca Nuova fumarole with UAV-MS-XPR3 ground test system in pack back configuration.
Figura 10 Misure raccolte con lo spettrometro di Massa UAV-MS-XPR3 presso Bocca Nuova.

trometer in very low concentrations (10 times smaller than H_2S). Also, the concentration of SO_2 was higher if condenser was removed (which indicates condenser removes part of the SO_2 gas when is been collected with bottles).

Figure 12 and Figure 13 show in situ direct MS sampling analysis in the calibrated multiple-ion mode from Bocca Nuova and Bocca Grande fumaroles taken with UAS-MS-XPR3 field test system. The concentration shows main volcanic gas to be CO_2 (tens of % levels), H_2S and SO_2 (10-100 ppmv) with water content removed. Note: H_2S and SO_2 ppm concentrations are referenced to left vertical axis (SO_2 ion trend is multiplied by 5 to better show values and correlation with other volcanic gases).

Intensity increases over time to reach a maximum due to the fact that the sample takes some time from the inlet of the probe to the MS to fully saturate the signal at the MS end. Also the exposure was relatively short without reaching steady state and for this reason MS graph looks like a chromatograph.

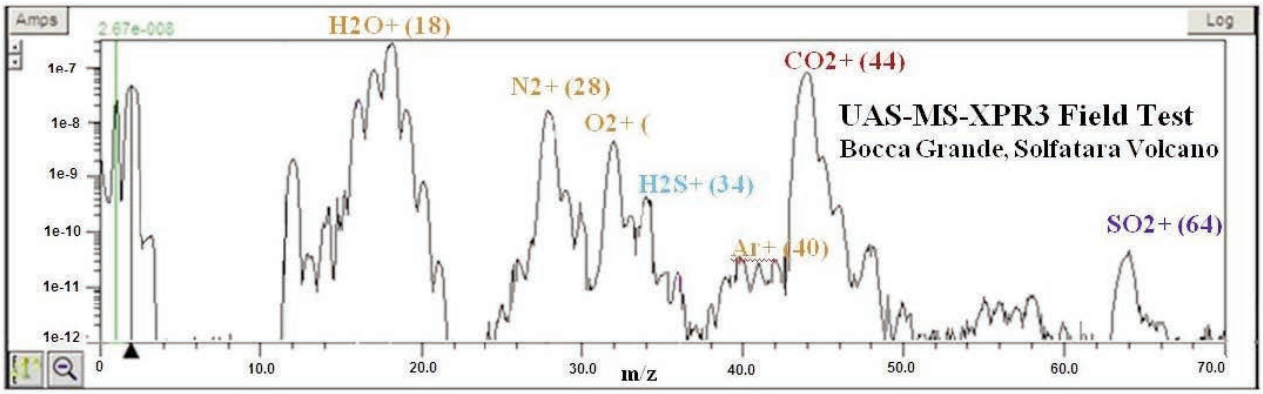

Figure 11 UAV-MS-XPR3 field test spectrum of Bocca Grande Fumarole, showing the presence of H_2O and CO_2 as main gases emitted and revealing the presence of H_2S and SO_2 as trace gases in tens of ppm concentration besides some air contamination (N_2, O_2, Ar peaks) (From JASMS Feb2015 edition).
Figura 11 Risultati ottenuti con lo spettrometro UAV-MS-XPR3 presso la fumarola Bocca Grande, mostranti la presenza di H_2O e CO_2 come gas principali emessi e rivelando la presenza di H_2S e SO_2, come tracce di gas in decine di ppm oltre qualche contaminazione dell'aria (N_2, O_2, picchi Ar) (Da JASMS feb edizione 2015).

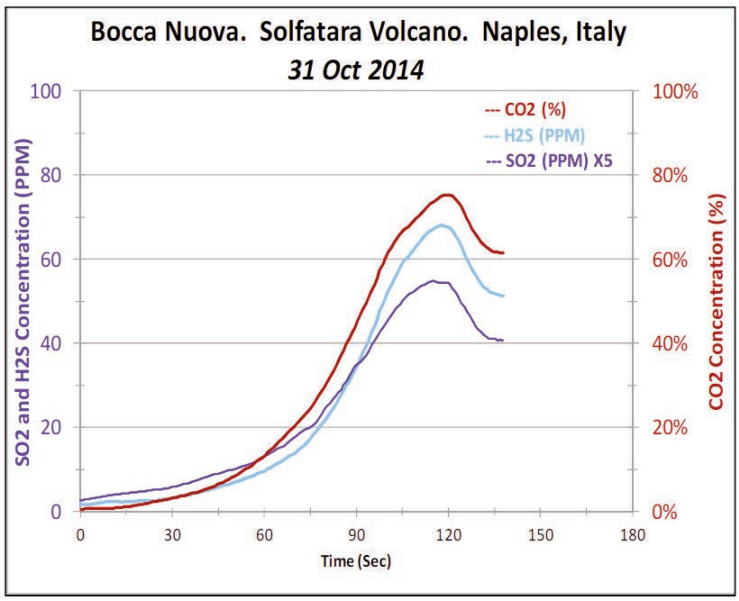

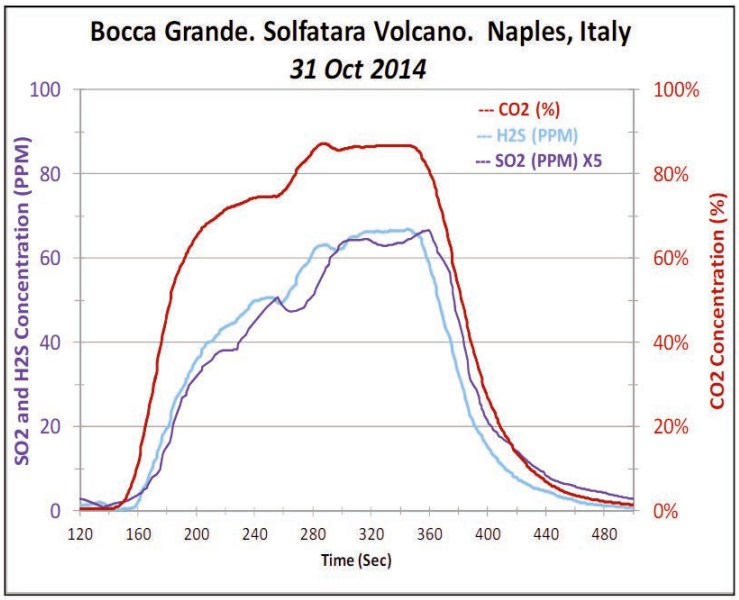

Figure 12 UAV-MS Field Test Results SO_2 and H_2S concentration at Bocca Nuova Fumarole. CO_2 concentration in percentage levels are referenced in right vertical axis.
Figura 12 Concentrazioni di SO_2 e H_2S presso la fumarola Bocca Nuova misurate con UAV-MS. Le concentrazioni in percentuale di CO_2 sono riportate sull'asse verticale destra.

Figure 13 UAV-MS Field Test Results SO_2 and H_2S concentration at Bocca Grande Fumarole.
Figura 13 Concentrazioni di SO_2 e H_2S presso la fumarola Bocca Grande misurate con UAV-MS.

Measurements of soil CO_2 flux and CO_2 concentration in air

The survey included the measurement of soil CO_2 flux and concentrations in air of CO_2 and H_2S, when possible, and soil temperature at 10cm depth. The location of the measurement points is reported in Figure 14 and the data in Table 1.

Soil CO_2 fluxes were measured using an accumulation chamber equipments developed and calibrated c/o Perugia University laboratories which operate according to the accumulation chamber method described in detail in Chiodini et al. [1998]. The equipment consists of: 1) a metal cylindrical vessel (the chamber, AC), 2) an Infra-Red (IR) spectrophotometer, 3) an analog-digital (AD) converter, and 4) a palmtop computer. The AC of a volume of about 2.8 L and are inside equipped with ring-shaped perforated manifold reinjecting the circulating gas to ensure the mixing of the air in the chamber. The IR spectrometers consists d LICOR Li-820 equipped with a sensor operating in the range 0-20,000 ppm of CO_2. The gas is circulated from the chamber to the IR and vice versa by a pump (~ 1L/m). The concentrations of the CO_2 in the gas inside the AC is acquired each 250 msec, converted by the AD and transmitted to a palmtop computer where is plotted in real time on a concentration vs time diagram. The ϕCO_2 is computed in real time on from the rate of CO_2 concentration increase in the chamber ($dCCO_2/dt$) considering the equation:

$$\phi CO_2 = cf \times dC_{CO2}/dt.$$

The proportionality factor (cf) between $dCCO_2/dt$ and the ϕCO_2 was determined before the survey by laboratory tests, during which ϕCO_2 values, typically from 10 to 10,000 g m-2 d-1, were measured on a "synthetic soil" made of dry sand (10 cm thick) placed inside a plastic box with an open top.

Point	Easting WGS84	Northing WGS84	T 10 cm depth (°C)	soil CO_2 flux (g/m^2d)	air H_2S (ppm)	air CO_2 mean @1.7m (ppm)	Standard deviation
1	427645	4519938	93.4	42853.6	nd	**3175**	**855**
2	427619	4519919	89.8	36650.4	nd	**980**	**385**
3	427645	4519921	92.6	10663.0	nd	**2428**	**1621**
4	427637	4519964	83.6	3118.8	nd	**473**	**67**
5	427619	4519918	94	31732.8	nd	**740**	**170**
6	427608	4519913	38.7	978.8	nd	**460**	**94**
7	427576	4519907	33.3	1581.2	nd	**338**	**60**
8	427572	4519921	76.1	934.3	nd	**547**	**133**
9	427579	4519936	60.6	165.8	nd	**391**	**73**
10	427551	4519939	57	2234.2	nd	**441**	**121**
11	427530	4519925	62.2	216.7	nd	**420**	**114**
12	427502	4519920	39.9	1071.7	nd	**392**	**39**
13	427485	4519895	39	482.7	nd	nd	nd
14	427482	4519906	37	1024.7	nd	nd	nd
15	427482	4519928	45.1	1215.9	nd	**389**	**72**
16	427496	4519939	77.8	13993.9	nd	**427**	**95**
17	427543	4519938	92.6	2208.5	8	**607**	**158**
18	427557	4519939	41.4	25.8	10	**597**	**148**
19	427610	4519953	46.3	821.2	7	**632**	**203**
20	427620	4519948	92.6	4446.4	17	**1110**	**625**

Table 1 Collected data.
Tabella 1 Elenco dei dati raccolti.

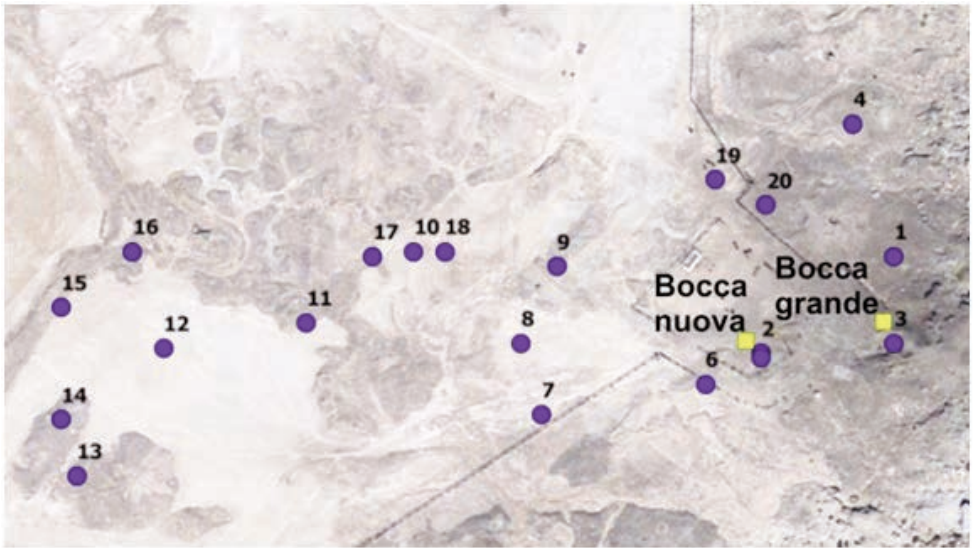

Figure 14 Location of measurements.
Figura 14 Punti di misura.

The cf factor was then computed as the slope of the linear best-fit line of ϕCO_2 vs. dC_{CO2}/dt.
The measurements of CO_2 air concentration were performed using an IR spectrometers LICOR Li-800 equipped with a sensor operating in the range 0-5,000 ppm of CO_2 connected to a pump with a flow rate of ~ 1L/m. The concentrations were recorded each 250 msec for a period varying between 10 and 50 sec. The mean value and the standard deviation is reported in Table 1.
The H_2S concentration were measured with a portable multigas XAM 7000 by Draeger equipped with an electrochemical sensor with a full scale of 1000 ppm.
Soil temperature were measured at the depth of 10 cm by the means of a thermocouple equipped with a metallic probe.

1.2 Thermal measurements

Two thermal cameras were used for the surface temperature measurements: a FLIR thermal imaging SC640 of Telecamere Termiche Mobili (TTM at INGV-OV) and a Thermotecnix VISIR640 of optical lab UF-8 (INGV-CNT). The measurements were carried out simultaneously with the two thermal cameras and thermocouples for a punctual measure (Figure 15).
The thermal camera FLIR SC640 is a high resolution (640 x 480 pixels), with thermal sensitivity of 0.06° C (+30° C) and an accuracy of ± 2° C (or ± 2% of reading). K-type thermocouple has been used measuring range from -200° C up to 1260° C with an error of about 0.1° C using a Fluke 52 II thermometer for the readout.
The Thermotecnix VISIR640 is a highly sensitive thermal camera (640 x 480 pixels) with a spectral range from 7.5 to 13 µm, an accuracy of ± 2° C (or ± 2% of reading) and a 60 mk thermal sensitivity.
Thermal measures collected by optical lab were performed only in daytime, while those collected by TTM were performed both in daytime and in nighttime. This has been done in order to estimate the effects of solar irradiation over the acquired data that may interfere with ther-

Figure 15 FLIR SC640, Thermotecnix VISIR640, Fluke 52 II with thermocouple of measurements K type (from left to right).
Figura 15 Camere termiche: FLIR SC640, Thermotecnix VISIR640, Fluke 52 II con termocoppia di misure di tipo K (da sinistra a destra).

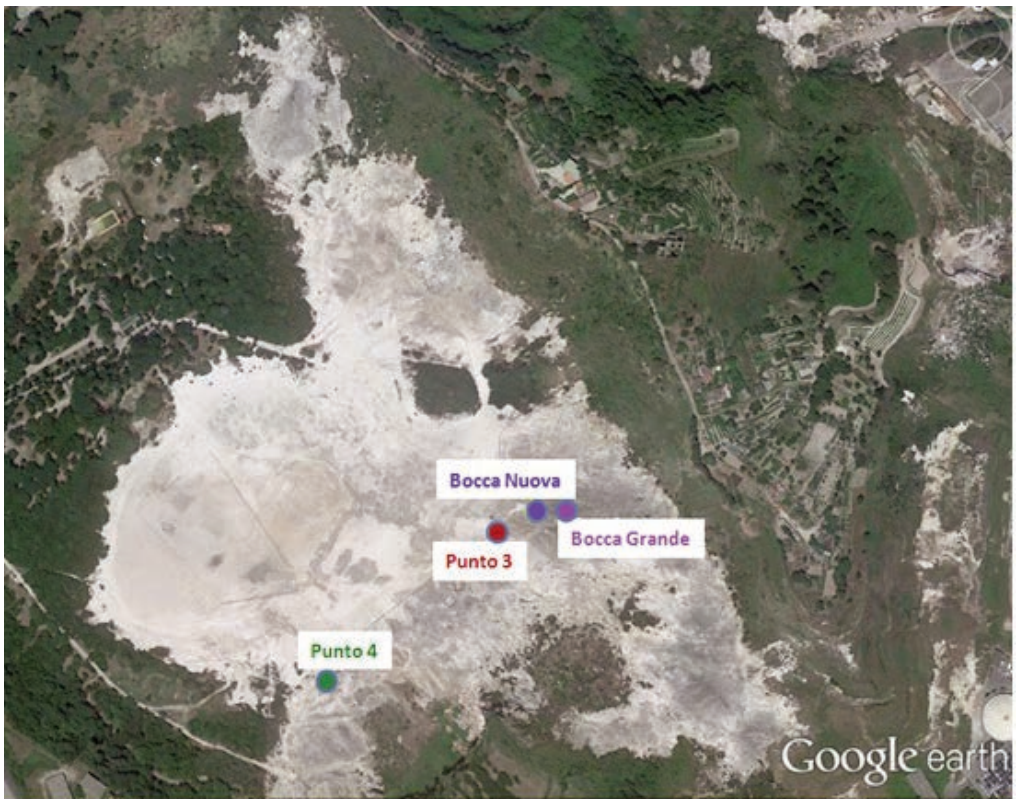

Figure 16 Sites of measures.
Figura 16 Ubicazione punti misura.

mal measurements. The comparison of night and day images showed that there are not substantial differences between the two measures. This is also due to the fact that the acquisition distances are small (in the order of few meters) and to the high temperatures of the sources. The small acquisition distances assures us that the attenuation effects of atmospheric temperature and humidity can be safely neglected.

The measures were focused on 4 areas identified and shown in Figure 16. They were chosen because they represent the main Solfatara thermal sources. They were measured in parallel using both thermal cameras in order to compare the performances of the instruments. Despite the fact that the sites have been measured at same time the field of view is slight different because the cameras were used by hand. This comparison represents a suitable test to acquire reliable data for validation and calibration activity. In the next figures (Figure 17-Figure 21) it is possible to consider how angle and viewing distance are significant factor in determining surface temperatures. When thermal imaging cameras are used within a few meters from fumaroles, the effect of integrated averaging radiance is reduced. Considering a viewing distance close to zero cameras would provide the highest resolution and the best resolved temperatures, but this is often impracticable or not safe for personnel performing analysis. However, appreciating how much resolution is required to obtain useable temperatures is important for quantitative analysis of data.

Figure 17 shows the thermal images of measurements at Bocca Nuova site, acquired at 10.50 (local time) on 30 October 2014. The thermal data acquired using FLIR SC640 were corrected considering in the thermal camera the atmospheric temperature values (T_{atm}) and humidity (U) measured with a thermo-hygrometer at the time of the measures. Measurement with K-type thermocouple has been collected in the same site and the value of temperature has been 144.7° C, quite comparable with the collected temperature acquired by means of proximal instruments (Figure 18).

This instrumental set up has been applied also on the next three sites.

Figure 19 shows the thermal images of measurements collected at Bocca Grande, acquired at 11.40 (local time). The atmospheric temperature is 25.4° C and humidity of 32%.

Figure 20 shows the thermal images of the measurements taken in Point 3 (Figure 16), acquired at 12.40 (local time). The atmospheric temperature is 22.9° C and humidity of 36%.

Finally, Figure 21 shows the thermal images of the measurements taken in Point 4 (Figure 16), acquired at 12.30 (local time). The atmospheric temperature is 22.9° C and humidity of 36%. This example highlights that different view angle causes significant variations in the temperatures measured by thermal imaging cameras.

Figure 22 shows the nighttime thermal images sensed at selected sites, by FLIR SC640. The atmospheric temperature values (T_{atm}) and humidity (U) measured with a thermo-hygrometer at the time of the measures and whose values are given in the respective figures.

Moreover thanks to the installation of a network of remote sensing systems, based on infrared thermal technology (permanent stations of IRT TV camera), on the Solfatara vol-

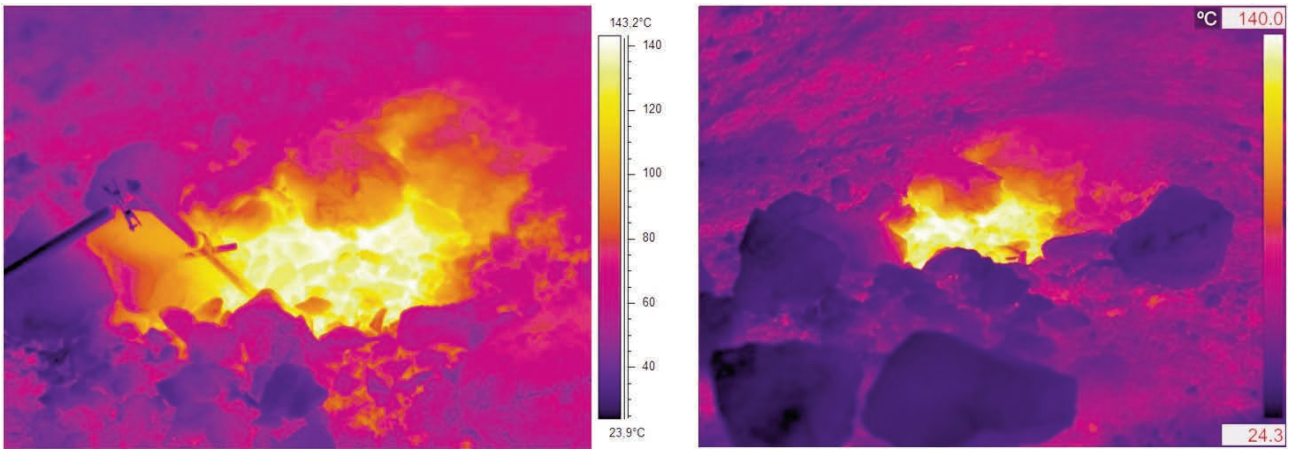

Figure 17 Bocca Nuova; thermal image acquired using FLIR SC640 (left), Thermotecnix VISIR640 (right).
Figura 17 Bocca Nuova; immagine termica acquisita con FLIR SC640 (sinistra), Thermotecnix VISIR640 (destra).

Figure 18 Bocca Nuova: temperature acquired using K-type thermocouple.
Figura 18 Bocca Nuova; temperatura acquisita con termocoppia K-type.

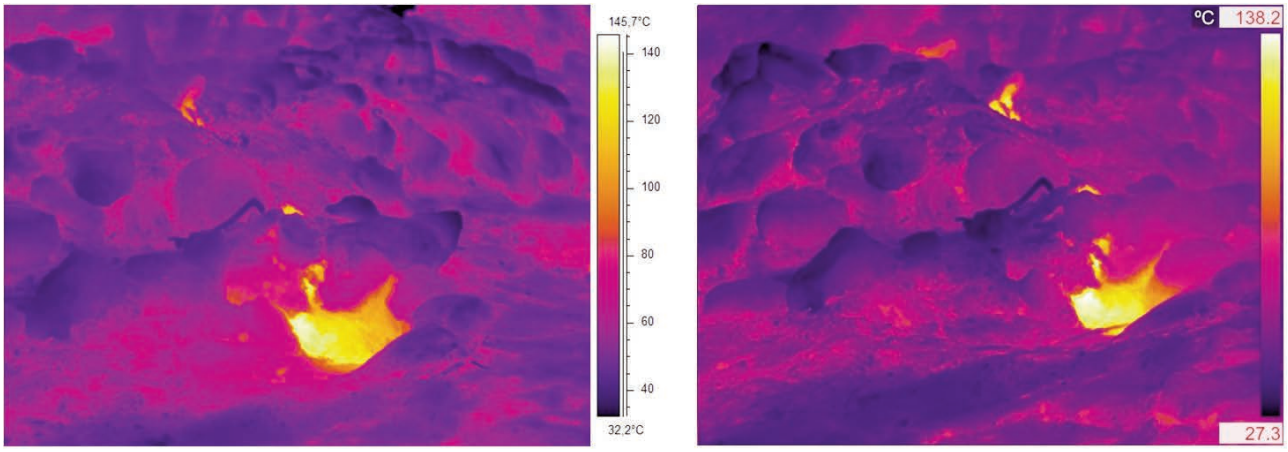

Figure 19 Bocca Grande; thermal image acquired using FLIR SC640 (left), Thermotecnix VISIR640 (right).
Figura 19 Bocca Grande; immagine termica acquisita con FLIR SC640), Thermotecnix VISIR640 (destra).

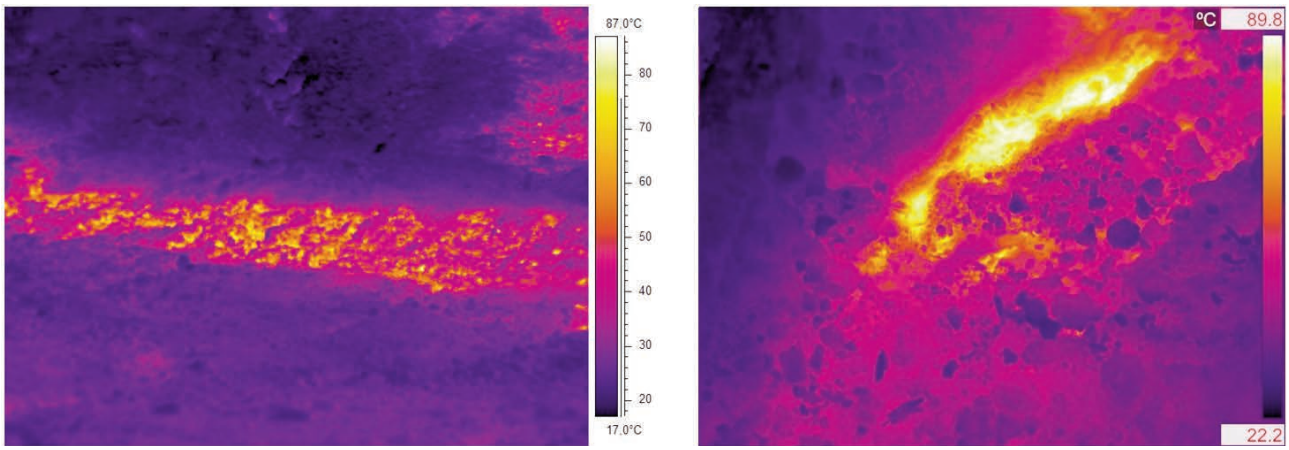

Figure 20 Point 3; thermal image acquired using FLIR SC640 (left), Thermotecnix VISIR640 (right).
Figura 20 Punto 3; immagine termica acquisita con FLIR SC640 (sinistra), Thermotecnix VISIR640 (destra).

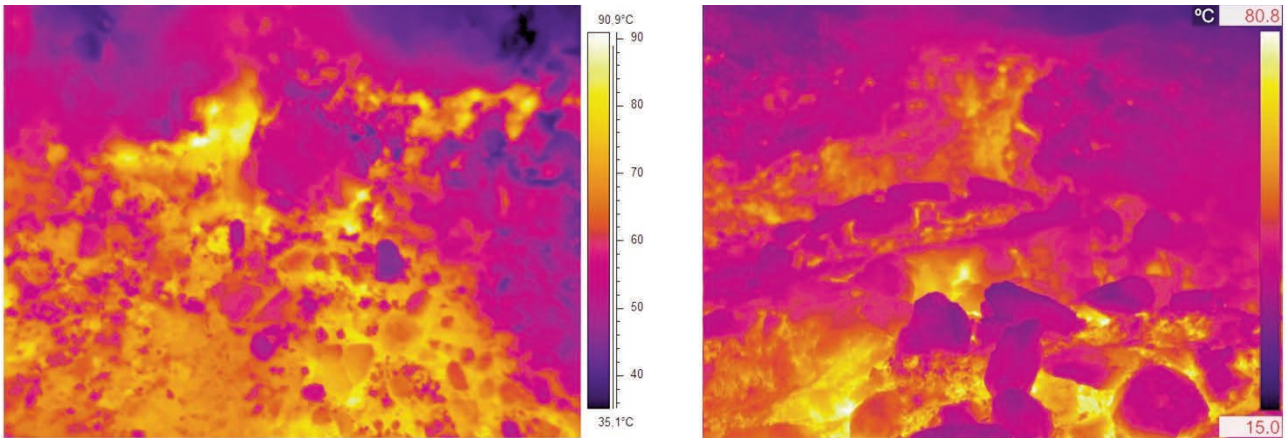

Figure 21 Point 4; thermal image acquired using FLIR SC640 (left), Thermotecnix VISIR640 (right).
Figura 21 Punto 4; immagine termica acquisita con FLIR SC640 (sinistra), Thermotecnix VISIR640 (destra).

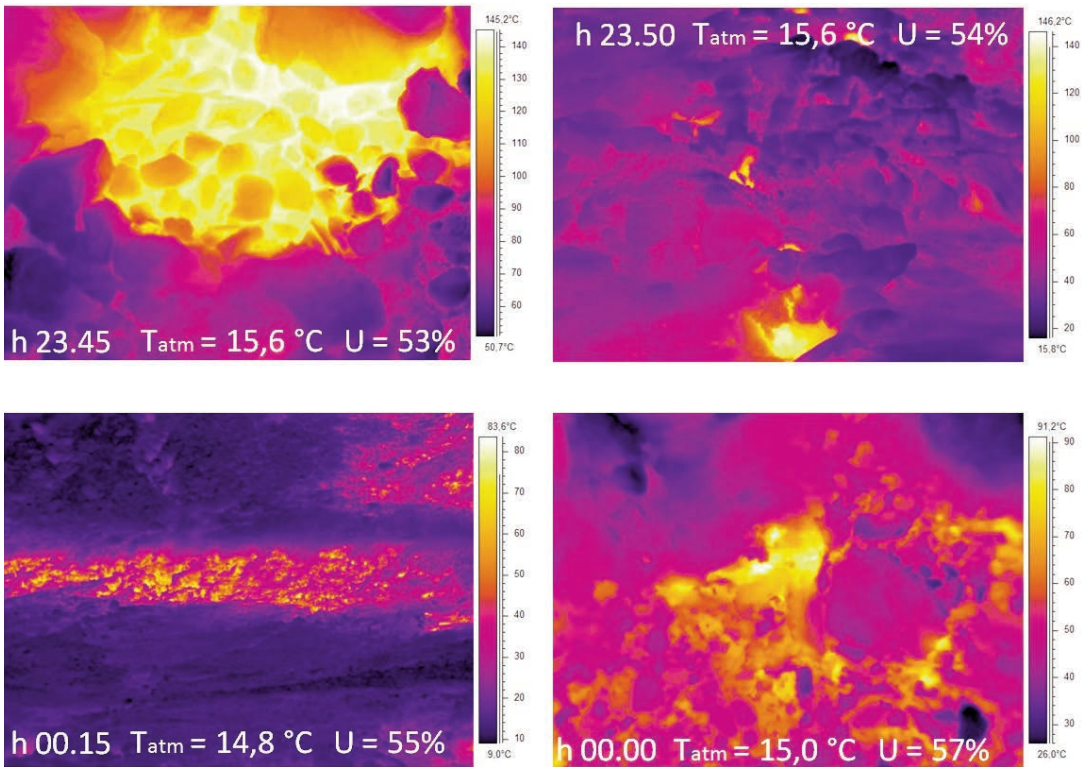

Figure 22 Bocca Nuova (a), Bocca Grande (b), point 3 (c) and 4 (d) ; thermal image acquired using FLIR SC640.
Figura 22 Bocca Nuova (a), Bocca Grande (b), punto 3 (c) e 4 (d); immagine termica acquisita con FLIR SC640.

cano it is possible the monitoring of the outgassing through the direct survey, and in real time, of the thermal anomalies of surface, Figure 23. This kind of measurement is useful for constant monitoring of surface temperature of fumaroles fields.

The IR cameras used at Solfatara are a FLIR SC325 (resolution 320x240 pixel) and a FLIR SC645 (resolution 640x480 pixels). The first one acquires scenes of the SE inner slope of Solfatara at the intersection of two active, SW-NE and NW-SE main faults where are located the major fumaroles (Bocca Grande e Bocca Nuova) (Figure 24, left) at an average distance of about 300 m from the IR camera. The station SF2 operative since June 2013 frames the inner slope of the northern sector (Figure 24, right).

Through the SF1 station the frame from 10.30 to 11.30 local time on the day 30 October has been acquired (Figure 25).

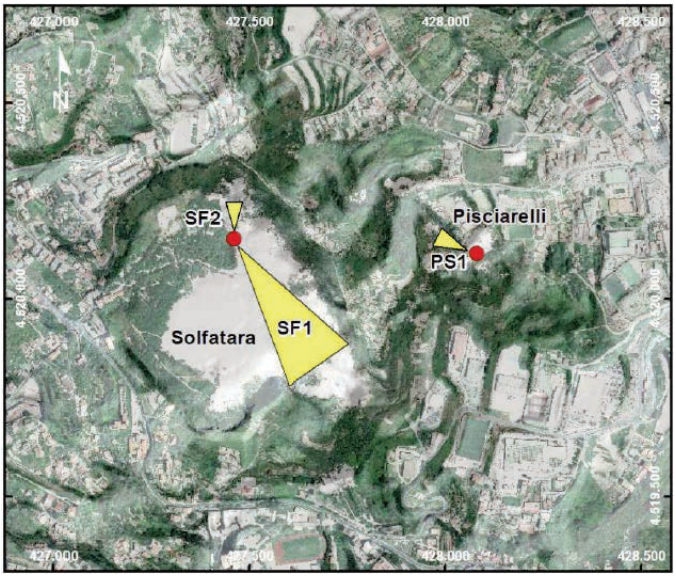

Figure 23 Location of fixed thermal camera.
Figura 23 Posizione della camera termica fissa.

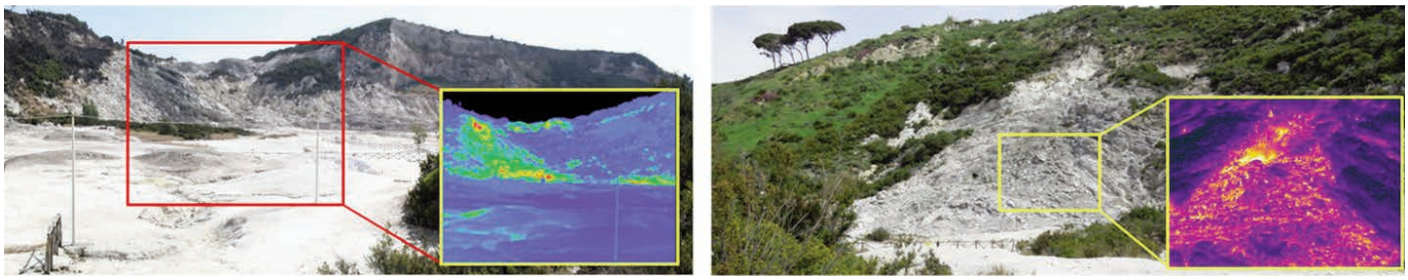

Figure 24 The SF1 station and relative acquisition area (left); SF2 station and relative acquisition area (right).
Figura 24 La stazione SF1 e relativa area di acquisizione (sinistra); stazione SF2 e relativa area di acquisizione (destra).

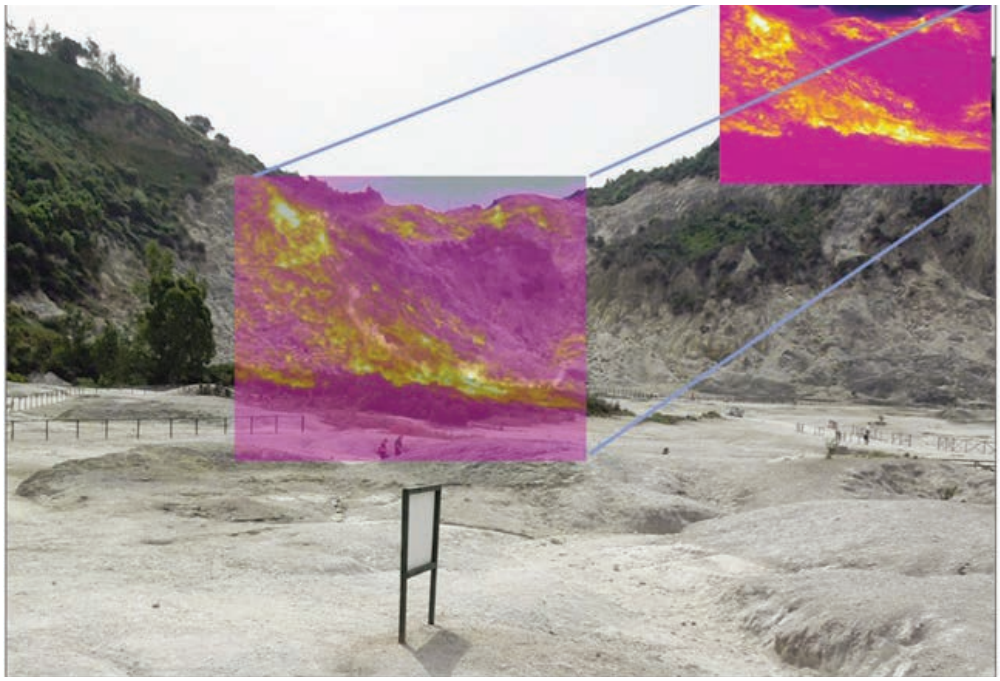

Figure 25 Thermal measurement collected by the fixed camera at Bocca Grande.
Figura 25 Misura della telecamera fissa inquadrante l'area di Bocca Grande.

1.3 Radiance and reflectance measures

Measures of radiances and reflectances on the Solfatara using the spectrometer ASD Field Spec Pro were collected at 30 October 2014. This instrument is a portable spectrometer with optical fiber used in field campaign and laboratory and operating in the spectral range 250-2500 nm with a spectral resolution of up to 3 nm. The instrument is equipped with an internal calibration system; calibration-operations are performed typically during the optimization at each measuring cycle or at any variations in environmental conditions. A laptop manages the acquisition instrument procedures allowing to measure the power of darkness and set the capture mode for the radiance or reflectance. Weather conditions during the field campaign were good, with clear skies. The measurements were made at different sites, whose position was detected by GPS (Figure 26.).

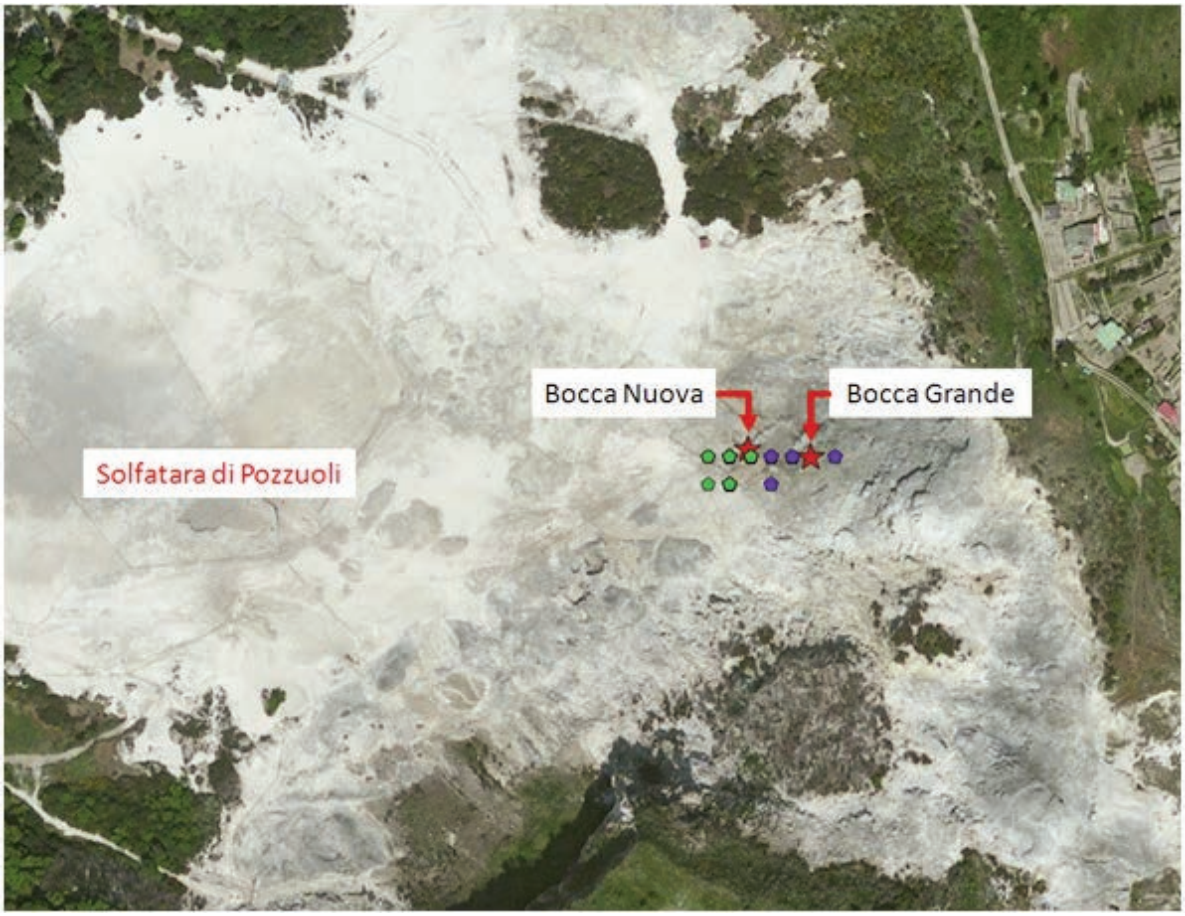

Figure 26 Measurement points acquired with ASD-FieldSpec; green and blue symbols: GPS points averaged for the positioning of the measures representative ASD FieldSpec 1700 measures on Bocca Nuova (green) and 1500 on Bocca Grande (blue).
Figura 26 Punti di misura acquisiti con l'ASD-FieldSpec; simboli verdi e blu: punti GPS mediati per il posizionamento delle misure ASD FieldSpec rappresentativi di 1700 misure su Bocca Nuova (verde) e 1500 su Bocca Grande (blu).

Site Name	Coordinates (Average)		N° of Measurements
	Latitude	Longitude	
Bocca Nuova	N 40° 49' 37"	E 14° 08' 30"	1700 (30 reflectance measurement)
Bocca Grande	N 40° 49' 37"	E 14° 08' 31"	1500

Table 2 GPS coordinates of the selected points and number of measurements collected by ASD-fieldSpec.
Tabella 2 Coordinate GPS dei punti selezionati e numero di acquisizioni raccolte con ASD-fieldSpec.

Table 2 shows the names of the measuring points and the number of spectra acquired for a total of 3200 acquired spectra. A photo reference was taken for each measured point (Figure 27 and Figure 28).

2. Satellite data

During this field campaign, the only satellite data available has been Landsat 8 acquired three days before the campaign. These data will be used for comparison. A second comparison will be done using ASTER data even if its acquisition has been on 26 September 2014 and considering low thermal variation in one month.

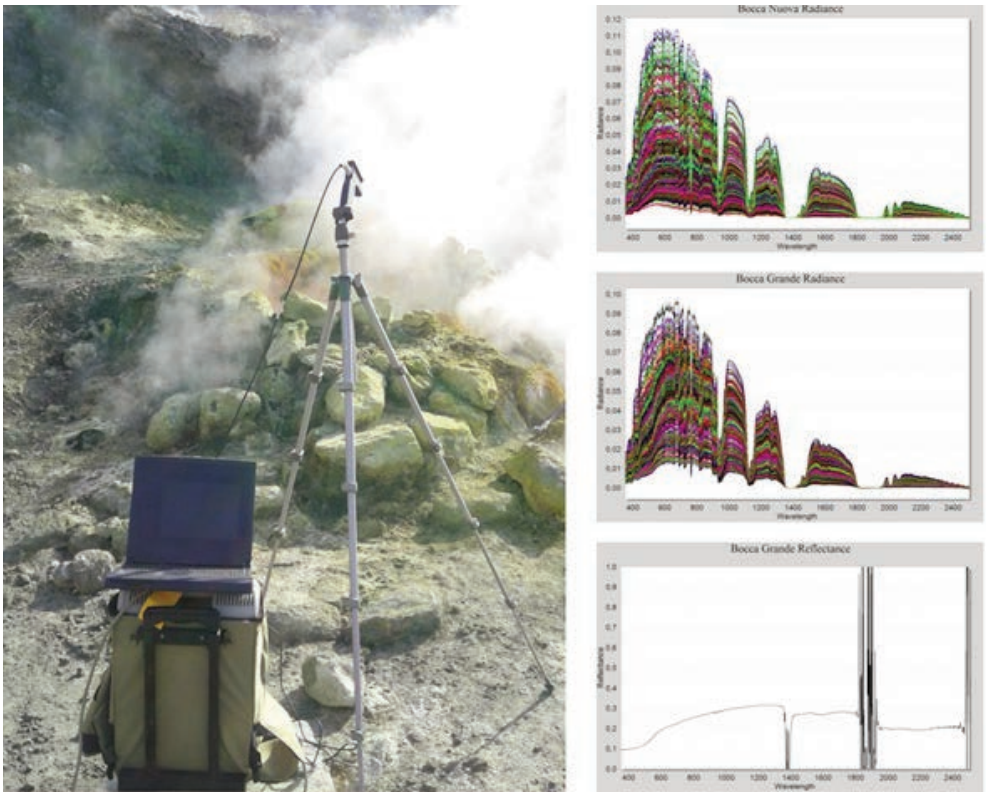

Figure 27 ASD-FieldSpec, radiance and reflectance measurement at Bocca Grande.
Figura 27 Misure di radianza acquisite con l'ASD-FieldSpec presso Bocca Grande.

Figure 28 Radiance measurements collected with ASD-FieldSpec at Bocca Nuova.
Figura 28 Misure di radianza acquisite con l'ASD-FieldSpec presso Bocca Nuova.

2.1 Landsat data

Landsat satellites have been collecting imagery of the Earth's surface since 1972 (Figure 29), creating a historical archive that is unmatched. The millions of scenes held in the USGS archives provide useful science to all users worldwide.Landsat 8 is the last satellite launched on February 11, 2013. It has two main sensors: the Operational Land Imager (OLI) and the Thermal Infrared Sensor (TIRS). OLI collects images using nine spectral bands in different wavelengths of visible, near-infrared, and shortwave light to observe a 185 kilometer (115 mile) wide swath of the Earth in 15-30 meter resolution covering wide areas of the Earth's landscape while providing sufficient resolution to distinguish features like urban centers, farms, forests and other land uses. TIRS images consist of two bands (10 and 11) useful in providing more accurate surface temperatures and are collected at 100 meters resolution. Approximate scene size is 170 km north-south by 183 km east-west (106 mi by 114 mi). In Figure 30 the Landsat8 band features are reported.

The Figure 31 shows the RGB combination by using the bands 4,3, and 2 and the gray scale of same acquisition considering the band 2 (482 nm), while the Figure 32 shows the at-satellite brightness temperature at band 10 and 11.

2.2 ASTER data

The ASTER sensor launched in December 1999 is one of five instruments on the Terra satellite, part of NASA's Earth Observing System (EOS). Terra follows a sun-synchronous nearly polar orbit with an equator crossing time of ~10:30 am/pm. The ASTER instrument has a 60 km swath width, which allows any point on the surface to be imaged at least once every 16 days. This sensor contains 14 spectral bands including three in the VNIR region (0.5 to 1.0 μm) with 15 m spatial resolution, six in the shortwave infrared (SWIR) region (1.0 to 2.5 μm) with 30 m spatial resolution, and five within the thermal infrared (TIR) region (8 to 12 μm) with 90 m spatial resolution [Kahle et al., 1991].

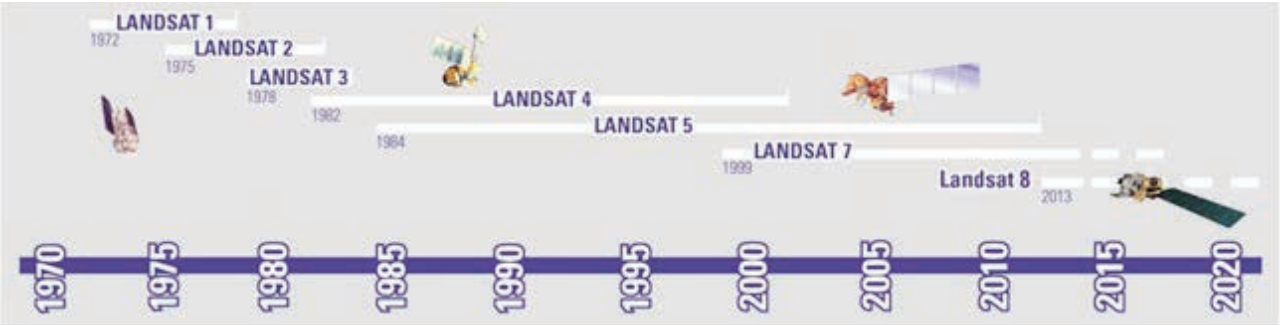

Figure 29 Landsat mission from 1972 till today.
Figura 29 Missione Landsat dal 1972 ad oggi.

Landsat 8 Operational Land Imager (OLI) and Thermal Infrared Sensor (TIRS) Launched February 11, 2013	Bands	Wavelength (micrometers)	Resolution (meters)
	Band 1 - Coastal aerosol	0.43 - 0.45	30
	Band 2 - Blue	0.45 - 0.51	30
	Band 3 - Green	0.53 - 0.59	30
	Band 4 - Red	0.64 - 0.67	30
	Band 5 - Near Infrared (NIR)	0.85 - 0.88	30
	Band 6 - SWIR 1	1.57 - 1.65	30
	Band 7 - SWIR 2	2.11 - 2.29	30
	Band 8 - Panchromatic	0.50 - 0.68	15
	Band 9 - Cirrus	1.36 - 1.38	30
	Band 10 - Thermal Infrared (TIRS) 1	10.60 - 11.19	100 * (30)
	Band 11 - Thermal Infrared (TIRS) 2	11.50 - 12.51	100 * (30)

Figure 30 Landsat 8 band features; * TIRS bands are acquired at 100 meter resolution, but are resampled to 30 meter in delivered data product. (http://landsat.usgs.gov/).
Figura 30 Caratteristiche delle bande del Landsat 8; * Le bandeTIRS sono acquisite a 100metri di risoluzione ma sono ricampionate a 30 metri (http://landsat.usgs.gov/).

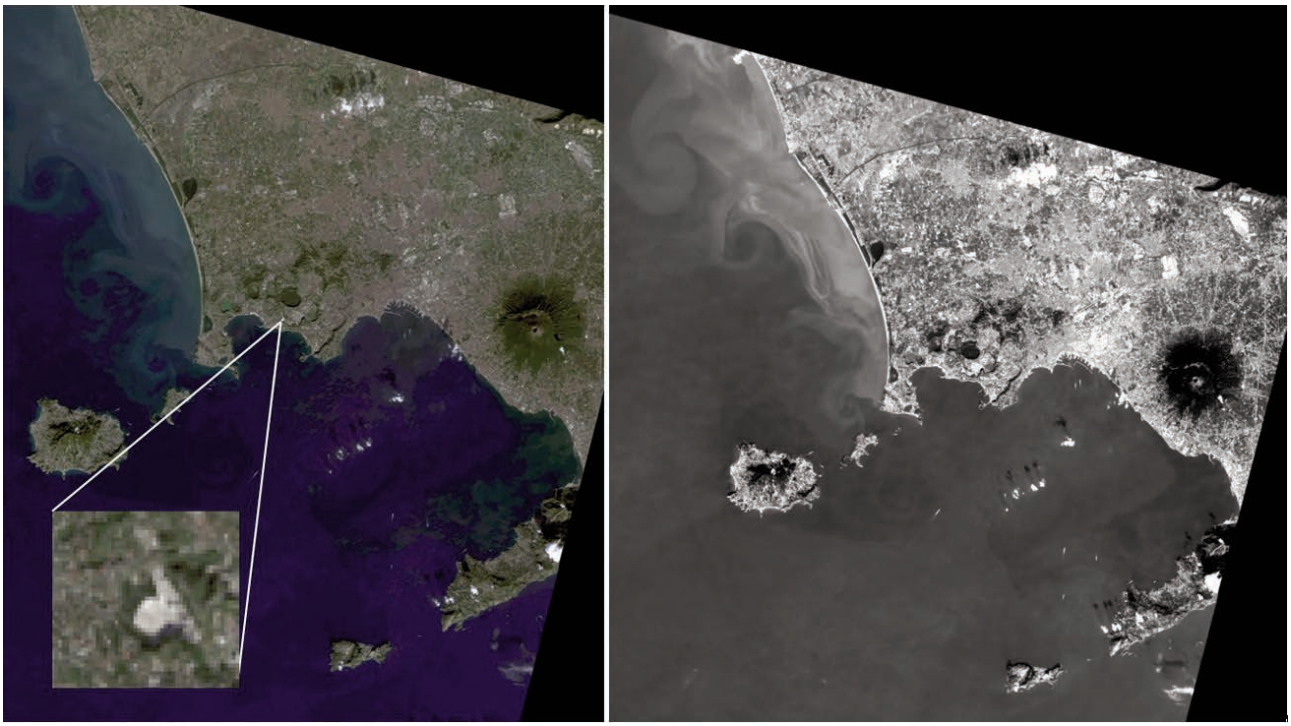

Figure 31 Landsat 8 image acquired 27 October 2014; RGB image (left, zoom of Solfatara area), grey scale of band 2 (482 nm, right).
Figura 31 Immagine Landsat8 acquisita il 27 ottobre 2014; immagine RGB (a sinistra, ingrandimento dell'area della Solfatara), immagine in scala di grigi della banda 2 (482nm, destra).

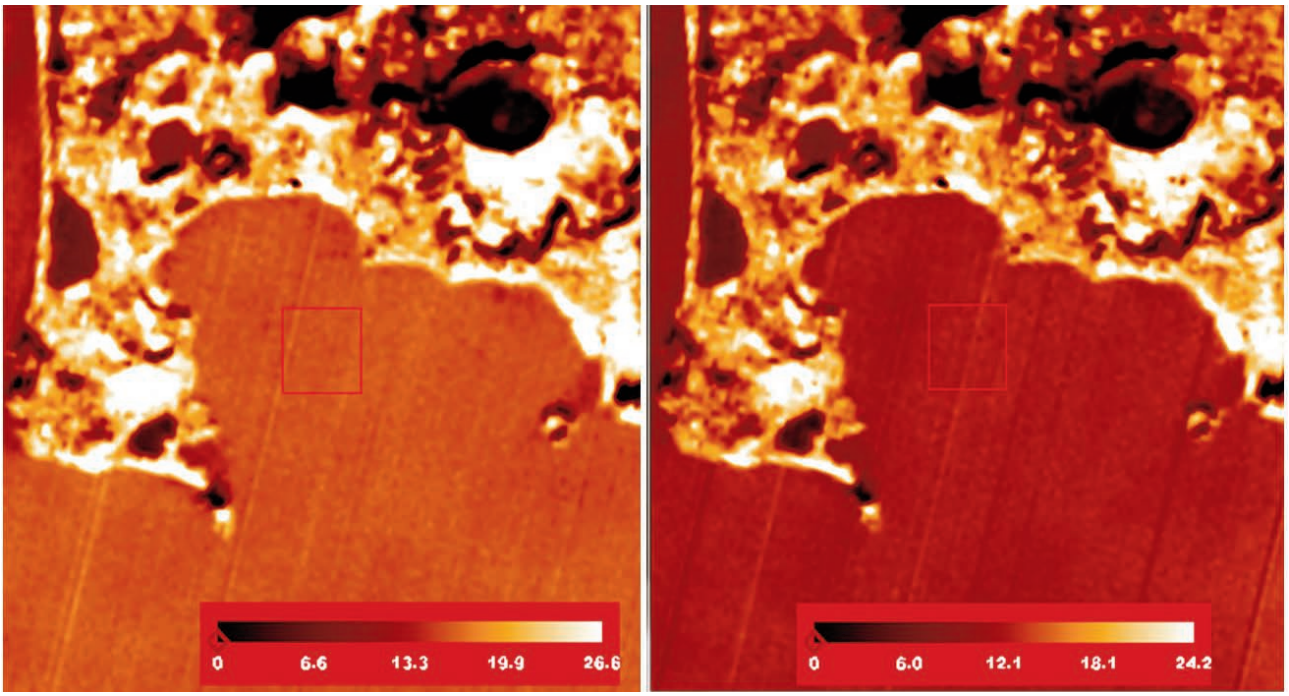

Figure 32 At-Satellite Brightness Temperature. The temperature is in °C.
Figura 32 Temperatura di brillanza al sensore. La temperatura è in °C.

ASTER is the first orbital sensor that provides publicly-available high-spatial resolution data with more than two bands in the TIR region. These data provide the ability to develop new methods for extracting the small scale compositional and temperature structure of the surface [Ramsey, 2002; Carter et al., 2009; Ramsey and Dehn, 2004].

Instrument	VNIR		SWIR		TIR	
	1	0.52-0.60	4	1.60-1.70	10	8.125-8.475
Bands and	2	0.63-0.69	5	2.145-2.185	11	8.475-8.825
Spectral Range (μm)	3N	0.78-0.86	6	2.185-2.225	12	8.925-9.275
			7	2.235-2.285	13	10.25-10.95
			8	2.295-2.365	14	10.95-11.65
			9	2.360-2.430		
Spatial Resolution	15m		30m		90m	
Swath Width	60km		60km		60km	
Cross Track Pointing	± 318km (± 24 deg)		± 116km (± 8.55 deg)		± 116km (± 8.55 deg)	
Quantisation (bits)	8		8		12	
Revisit Time	16 days		16 days		16 days	

Table 3 ASTER instrument characteristics [Yamaguchi et al., 1998].
Tabella 3 Caratteristiche di ASTER [Yamaguchi et al., 1998].

Date	T min (°C)	T mean (°C)	T max (°C)	Humidity (%)
26/09/2014	17	21.5	28.4	62
30/10/2014	14.5	18.9	22.7	87
31/10/2014	17.8	20.3	23	87

Unfortunately during the field campaign no ASTER data were available, but considering the ASTER data acquisition of 26th September 2014 (Figure 34) and the low thermal variation in one month, as showed in Figure 33, in the next months we will try to compare this data with Landsat 8 data.
The temperature is not an intrinsic property of the surface; it varies with the irradiance history and meteorological conditions. For this case we have considered the ASTER's night observation that shows well defined episodes of increasing thermal emission of crater thanks to a more uniform background temperature (Figure 35).

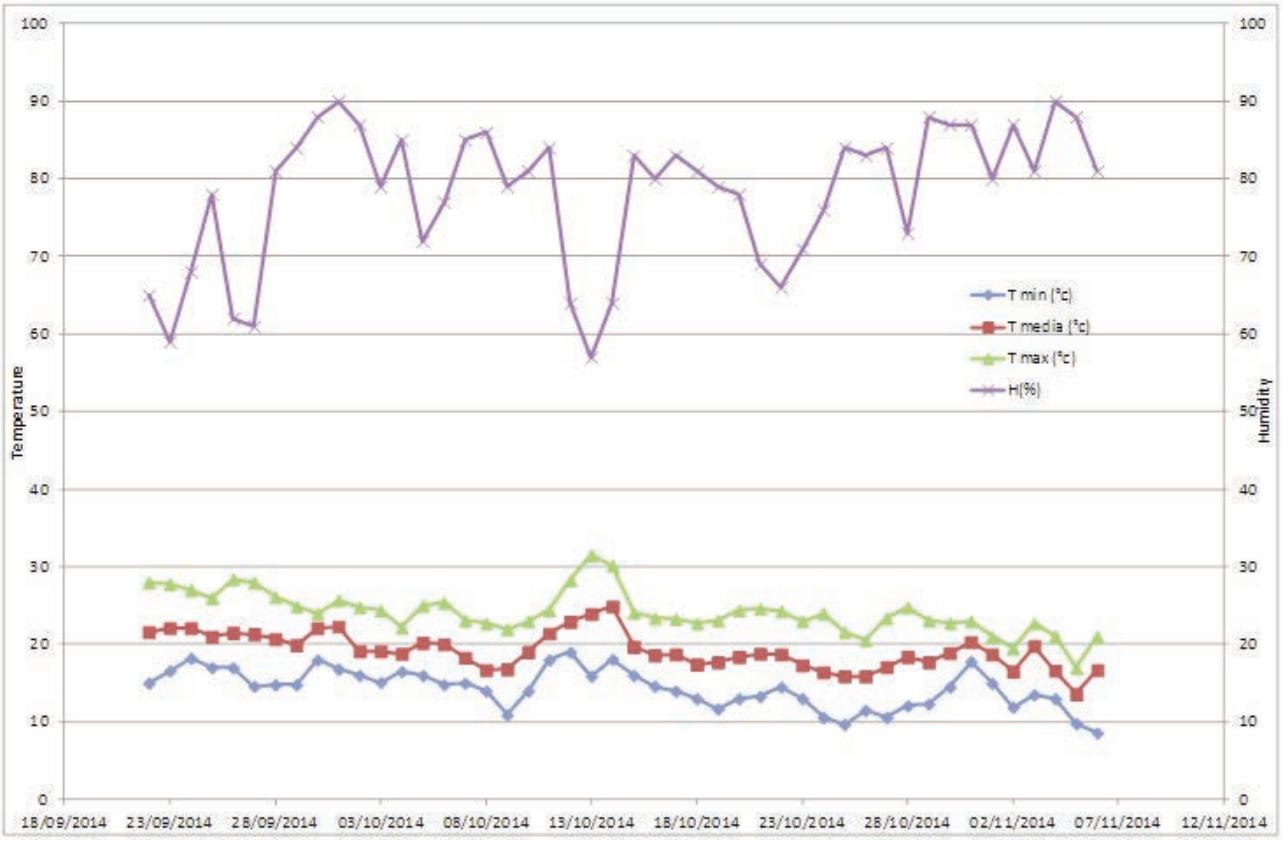

Figure 33 Temperature and humidity in the time period 23 September to 7 November 2014.
Figura 33 Temperatura e umidità nel periodo 23 Settembre - 7 Novembre 2014.

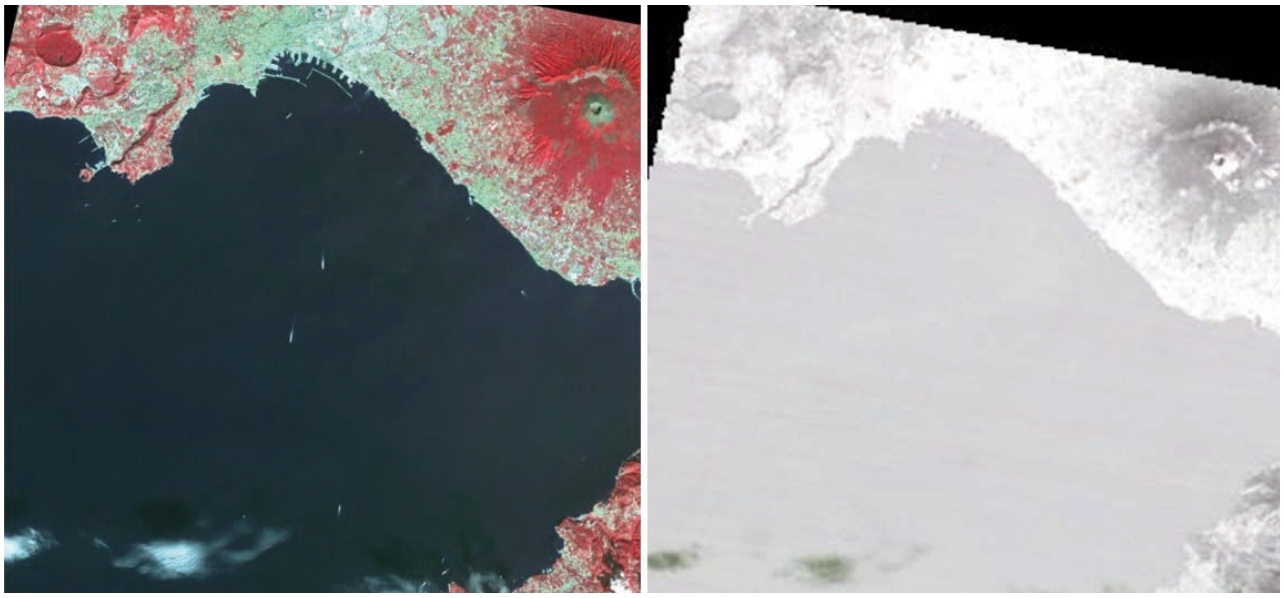

Figure 34 Daytime ASTER image acquired 26 September 2014; RGB image (left) in the visible region, gray scale image (right) in TIR region.
Figura 34 Immagine diurna di ASTER acquisita il 26 Settembre 2014; immagine RGB (sinistra) nella regione del visibile, immagine in scala di grigi (destra) nella regione TIR.

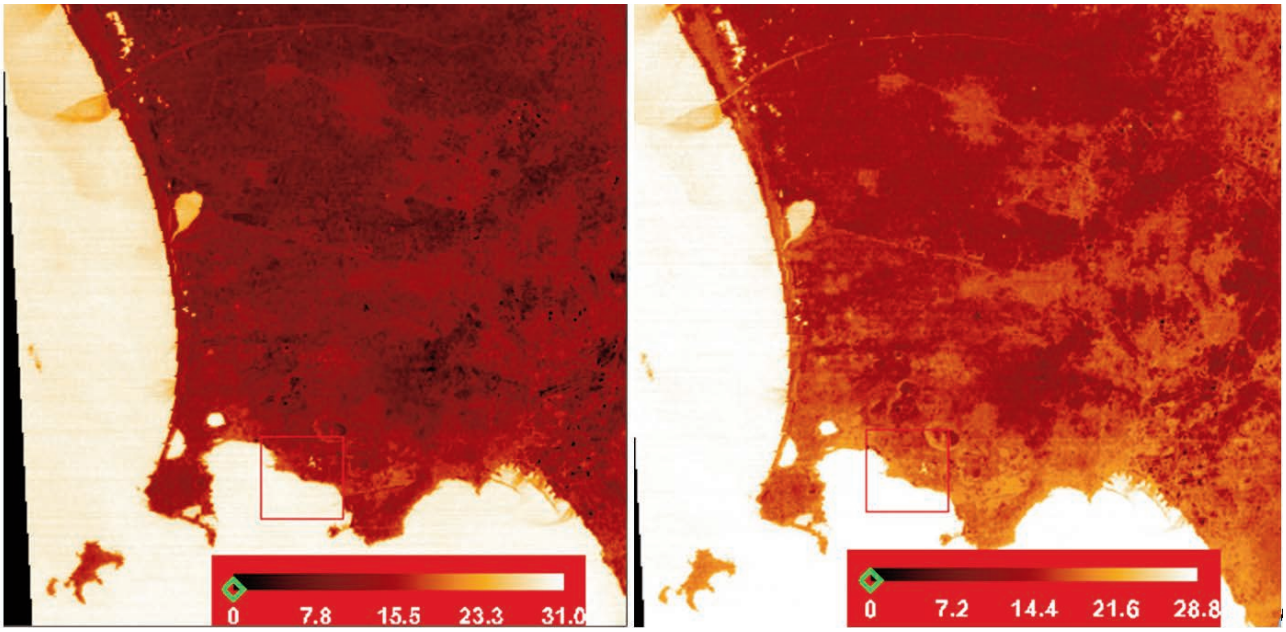

Figure 35 Nighttime ASTER image acquired 26 September 2014; Satellite Brightness Temperature at band 13 (left) and 14 (right). The temperature is in °C.
Figura 35 Immagine notturna di ASTER acquisita il 26 Settembre 2014; temperatura di brillanza al sensore, relative le bande 13 (sinistra) e 14 (destra). La temperatura è in °C.

Conclusions

Current work has the goal of describing testing new small, economical UAV platforms, with miniaturized instrument payloads, within a volcanic fumaroles in Solfatara volcano. The miniature multigas payload and the small mass spectrometer based unmanned aerial system (UAS) instrument were already used in the Costa Rica at Turrialba Volcano [Diaz et al., 2012; Pieri et al., 2013]. Collected measurements can provide in situ calibration and validation support for remote sensing observation of volcanic plumes and encourage the use of these instruments in dangerous area.

Concerning the thermal measurements, these preliminary data show that an inter-calibration between two hand held thermal cameras is always possible, providing that they have the same resolution. The effects due to distances, view angles and environmental parameters can be easily taken into account in order avoid unwanted errors. Moreover the use of IRT TV camera permanent stations offers a continuous, long-term volcanological monitoring by acquiring daily infrared images of fumaroles field providing a temperature time series suitable for constant monitoring of surface temperatures of fumaroles fields. These fumaroles were also sensed by using portable spectro-radiometer in order to verify the capability of such instruments to detect different gases composing degassing fumaroles.

All information collected during the campaign will be used for further analysis; a new measurement campaign is planned at Vulcano Island in order to verify the instrument portability in areas less easy to access.

Acknowledgements

With this report we want to thank all colleagues for the hospitality, and the great support provided during the visit of Prof. Jorge Andres Diaz and Dr. Dave Pieri at INGV-OV and during the field campaign at Solfatara.

In particular we thank Elena Cubellis and Maria Ilaria Pannaccione Apa for their help throughout the organizational phase of the seminary and the visit of foreign colleagues. A special thanks to Stefano Caliro and all the staff of the laboratory that allowed Prof Andres Diaz of the assembly and calibrate the equipment, the Rete Mobile of Centro Nazionale Terremoti and Milena Moretti for providing technical equipment in support of the campaign. We thank all the groups who helped with the different measures to complete the test and especially Giovanni Chiodini. A heartfelt thanks to Giuseppe Vilardo for measurements of thermal fixed camera.

Finally we thank Francesco "Ciskie" Malafarina for photographic material collected during the measurement campaign.

References

Barberi F., Corrado G., Innocenti F. and Luongo G., (1984). *Phlegraean Fields 1982-1984: brief chronicle of a volcano emergency in a densely populated area.* Bull. Volcanol. 47, 175-185.

Chiodini G., Cioni R., Guidi M., Raco B. and Marini L., (1998). Soil CO_2 *flux measurements in volcanic and geothermal areas.* Appl. Geochem., 13, 543-552.

Diaz J.A., Pieri D., Wright K., Sorensen P., Kline-Shoder R., Arkin C.R., Fladeland M., Bland G., Buongiorno M.F., Ramirez C., Corrales E., Alan A., Alegria O., Diaz D. and Linick J., (2015). *Unmanned aerial mass spectrometer systems for in-situ volcanic plume analysis.* J. Am. Soc. Mass. Spectrom. 26(2): 292-304. doi: 10.1007/s13361-014-1058-x. Epub 2015 Jan 15.

Diaz J.A., Morris G.A., Selkirk H.B., Krotkov N.A., Pieri D. C. & Corrales E., (2012). *In situ detection of SO2 plumes in Costa Rica from Turrialba Volcano using balloon-borne sondes*. In: Proceedings of AGU 2012 Fall Meeting, 3–7 December, San Francisco, CA. American Geophysical Union, Washington, DC, Abstract A53Q-0433. http://landsat.usgs.gov/

Pieri D., Diaz J.A., Bland G., Fladeland M., Madrigal Y., Corrales E., Alegria O., Alan A., Realmuto V., Miles T. and Abtahi A., (2013). *In situ observations and sampling of volcanic emissions with NASA and UCR unmanned aircraft, including a case study at Turrialba Volcano, Costa Rica*. The Geological Society of London 2013, Geological Society, London, Special Publications, 380, 321–352. http://dx.doi.org/10.1144/SP380.13

Rosi M. and Santacroce R., (1984). *Volcanic hazard assessment in the Phlegrean Fields: a contribution based on stratigraphic and historical data*. Bull. Volcanol. 47, 359-370.

Rosi M. and Sbrana A., (1987). *Description of mapped products.* In: Rosi, M., Sbrana, A. (Eds.), Phlegrean Fields. Quaderni de 'La ricerca scientifica', Consiglio Nazionale delle Ricerche, Roma.

Vito M.A., Lirer L., Mastrolorenzo G. and Rolandi0 G., (1987). *The 1538 Monte Nuovo eruption (Campi Flegrei, Italy)*. Bull. Volcanol. 49, 608-615.

Index

ISSN 1590-2595

Quaderni di Geofisica

http://istituto.ingv.it/l-ingv/produzione-scientifica/quaderni-di-geofisica/

I Quaderni di Geofisica coprono tutti i campi disciplinari sviluppati all'interno dell'INGV, dando particolare risalto alla pubblicazione di dati, misure, osservazioni e loro elaborazioni anche preliminari, che per tipologia e dettaglio necessitano di una rapida diffusione nella comunità scientifica nazionale ed internazionale. La pubblicazione on-line fornisce accesso immediato a tutti i possibili utenti. L'Editorial Board multidisciplinare garantisce i requisiti di qualità per la pubblicazione dei contributi.

ISSN 2039-7941

rapporti tecnici INGV

http://istituto.ingv.it/l-ingv/produzione-scientifica/rapporti-tecnici-ingv/

I Rapporti Tecnici INGV pubblicano contributi, sia in italiano che in inglese, di tipo tecnologico e di rilevante interesse tecnico-scientifico per gli ambiti disciplinari propri dell'INGV. La collana Rapporti Tecnici INGV pubblica esclusivamente on-line per garantire agli autori rapidità di diffusione e agli utenti accesso immediato ai dati pubblicati. L'Editorial Board multidisciplinare garantisce i requisiti di qualità per la pubblicazione dei contributi.

ISSN 2039-6651

miscellanea INGV

http://istituto.ingv.it/l-ingv/produzione-scientifica/miscellanea-ingv/

La collana Miscellanea INGV nasce con l'intento di favorire la pubblicazione di contributi scientifici riguardanti le attività svolte dall'INGV (sismologia, vulcanologia, geologia, geomagnetismo, geochimica, aeronomia e innovazione tecnologica). In particolare, la collana Miscellanea INGV raccoglie reports di progetti scientifici, proceedings di convegni, manuali, monografie di rilevante interesse, raccolte di articoli ecc..

Coordinamento editoriale e impaginazione
Centro Editoriale Nazionale | INGV

Progetto grafico e redazionale
Daniela Riposati | Laboratorio Grafica e Immagini | INGV Roma

Via di Vigna Murata, 605
00143 Roma
Tel. +39 06518601 Fax +39 065041181

http://www.ingv.it

Istituto Nazionale di Geofisica e Vulcanologia